Microbubbles for Acoustically Mediated Drug Delivery to the Inner Ear

Charlotte Jeanneau, Fabrice Micaletti, Damien Fouan, Valérie Schubnel, Cédric Chauvierre, John Galvin, Jean-Michel Escoffre, David Bakhos

MICROBUBBLES FOR ACOUSTICALLY MEDIATED DRUG DELIVERY TO THE INNER EAR

Charlotte Jeanneau[1, 2], Fabrice Micaletti[1, 2], Damien Fouan[1], Valérie Schubnel[1], Cédric Chauvierre[3], John J. Galvin 3rd[4], Jean-Michel Escoffre[1,5], David Bakhos[1, 2]

[1]*Université de Tours, INSERM, Imaging Brain & Neuropsychiatry iBraiN U1253, 37032, Tours, France*

[2]*ENT and Cervico-Facial Surgery Department, University Hospital Center of Tours, 37044 Tours, France*

[3]*Université Paris Cité, Université Sorbonne Paris Nord, UMR-S U1148 INSERM, Laboratory for Vascular Translational Science (LVTS), F-75018, Paris, France*

[4]*House Institute Foundation, 2100 W 3rd Street, Suite 111, Los Angeles, CA 90057, USA*

[5]*CHRU de Tours, INSERM, CIC Tours CIC1415, 37044, Tours, France*

Corresponding authors

Charlotte Jeanneau
Service d'ORL et Chirurgie Cervico-Faciale, CHU Tours, 2 boulevard Tonnellé, 37044 Tours, France
Tel: +33 247 474 785. Fax: +33 247 473 600
E-mail: charlottejeanneau@orange.fr

Jean-Michel Escoffre
Université de Tours, INSERM, Imaging Brain & Neuropsychiatry iBraiN U1253, 37032, Tours, France
Tel: +33 247 366 191
E-mail : jean-michel.escoffre@inserm.fr

Abstract

The blood-labyrinth barrier (BLB) is a selective endothelial barrier that maintains the homeostasis of the inner ear and protects it against toxic molecules and pathogens. This highly selective barrier represents a significant challenge for the delivery of therapeutic agents to the inner ear. To overcome this issue, various drug delivery methods have been developed. Among these modalities, microbubble-assisted ultrasound is an innovative and promising method for the non-invasive, targeted and efficient delivery of therapeutic agents through the round window membrane. The safety and the efficacy of this physical modality is strongly dependent of physiological properties of the targeted tissue, the pharmacological properties of the therapeutic molecules, the ultrasound parameters but also microbubble-related properties. The present review focuses on the current state of MB formulations and their use for the acoustically mediated inner ear drug delivery.

Keywords: sonoporation; microbubbles; ultrasound; drug delivery; inner ear; round window membrane.

49

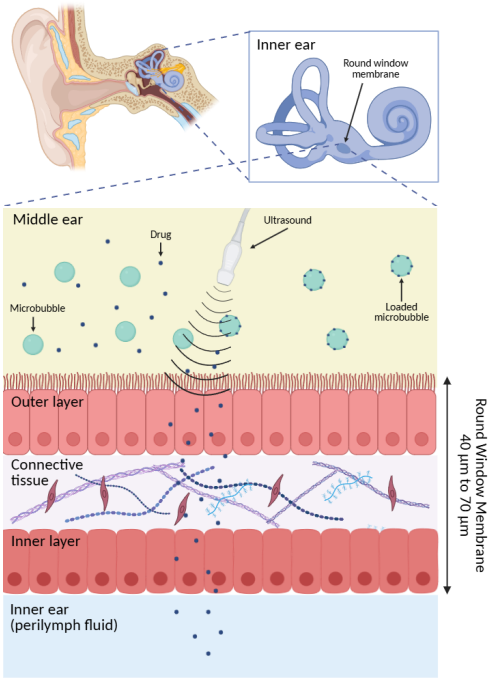

Figure 1: Principle of drug delivery using MB-assisted US through the round window membrane. Made with BioRender.

Abbreviations:

AAV: Adeno-associated virus

BLB: Blood-labyrinth barrier

Biotin-FITC: Biotin fluorescein isothiocyanate

CS-AuNPs: Nano-chitosan capped gold nanoparticles

C_3F_8: Octafluoropropane

C_4F_{10}: Perfluorobutane

DPPA: Di-palmitoyl-phosphoric acid

5000-DPPE: 500-Di-palmitoyl-phosphatidylethanolamine

DPPC: Di-palmitoyl-phosphatidylcholine

DPPG: Di-palmitoyl-phosphoglycerol

DSPC: Di-stearoyl-phosphatidyl-choline

DSPE-PEG 2000: Di-stearoyl-phosphoryl-ethanolamine-polyethylene glycol 2000

HEI-OC1: Mouse cochlear hair cell line

HEPS: Hydrogenated egg yolk phosphatidylserine

HSA: Human serum albumin

IGF-1: Insulin-like growth factor-1

MB: Microbubble

MM1: Vevo MicroMarker-1

PEG: Polyethylene glycol

P407: Poloxamer 407

PRISMA: Preferred reporting items for systematic review and meta-analysis

RNA: Ribonucleic acid

RWM: Round window membrane

SNHL: Sensorineural hearing loss

Cy3 siNOX4: Cellular uptake of cyanine 3 small interfering NADPH oxidase 4

SF_6: Sulfur hexafluoride

US: Ultrasound

INTRODUCTION

The inner ear is a complex and essential organ of the auditory system, playing a crucial role in both hearing and balance. It consists of two main structures: the cochlea and the vestibule. The inner ear can be susceptible to various pathologies, particularly sensorineural hearing loss (SNHL), which is the most common sensory deficit worldwide. It is estimated that approximately 430 million people globally are affected, with projections rising to 700 million by 2050 [1].

The management of hearing loss is a critical concern within the medical community due to its significant impact on daily life. Hearing loss can profoundly affect communication, education, and psychosocial well-being of patients. Additionally, the economic burden associated with hearing loss presents a substantial societal challenge [2]. Currently, the rehabilitation of auditory function in cases of SNHL relies on various therapeutic modalities, including hearing aids and cochlear implants. These treatments are selected based on the severity and type of hearing loss. However, some are not suitable for all individuals and may have limitations regarding accessibility and efficacy. Currently, there are no approved pharmacological treatments that specifically target sensory dysfunction of the inner ear or promote sensory recovery [3]. Recent research has been directed at investigating novel approaches, such as gene therapy and hair cell regeneration within the inner ear [4].

Much research has been directed at delivering therapeutic agents to the inner ear to protect or restore auditory function. Several administration routes of these agents have been investigated, including systemic delivery via intravenous or oral routes, as well as transtympanic and intracochlear injections. Transtympanic injection is commonly used in clinical practice because it is less invasive compared to the intracochlear administration. In addition, transtympanic injection allows for local administration of high drug concentrations while minimizing systemic exposure and side effects. However, this delivery method presents several challenges due to the anatomical and physiological complexity of the inner ear. The inner ear is located deep in the dense temporal bone, which limits direct access. The first anatomical barrier is the tympanic membrane. Once the therapeutic agent reaches the middle ear, its volume is further reduced due to partial drainage through the auditory tube. Ultimately, drug delivery to the inner ear primarily occurs via passive diffusion across the round window membrane (RWM). This diffusion process is significantly restricted by several factors, including the presence of the blood-labyrinth barrier (BLB) [5,6]. The RWM consists of three cellular layers formed by endothelial cells connected by tight junctions, which severely limit the diffusion of many therapeutic agents. The molecular size, the concentration, the lipophilicity, and the electrical charge of these molecules strongly influence their permeability through the RWM.

To overcome limitations of current treatments, innovative modalities, such as microbubble-assisted ultrasound (MB-assisted US) have been developed and validated to enhance drug delivery to target organs. This modality (*i.e.,* “sonoporation” or “sonopermeation”) relies on the combined use of US and MB to increase the membrane permeability of biological barriers (*e.g.,* BLB, blood-tumor barrier, plasma membrane, *etc.*) to therapeutic agents and to facilitate their delivery to target cells and tissues [7]. The exposure of MBs to US waves induces their volumetric oscillations, which, depending on the cavitation regime (stable *versus* inertial), generate multiple local acoustic phenomena (*e.g.,* push/pull forces, microstreaming, shock waves, and microjets) near biological barriers. These acoustic phenomena increase the native permeability of these barriers through the

stimulation of intracellular (*i.e.,* formation of membrane pore, stimulation of endocytosis), paracellular (*i.e.,* disruption of tight junctions) and transcellular pathways (*i.e.,* transcytosis) [8,9]. MB-assisted US is a promising modality for the delivery of wide range of therapeutic agents (*e.g.,* nucleic acids, chemotherapeutics, antibiotics, antibodies, immune and stem cells). These therapeutic agents can be either coadministered or sequentially administered with MBs or loaded within MB core or on/within the MB shell. The exposure of drug-loaded MBs to US can trigger drug release from MBs in a site-specific manner. This US modality is undergoing preclinical and clinical investigations in multiple medical fields, including oncology [10], neurology [11] and cardiology [12,13]. More recently, drug delivery using MB-assisted US has been reported for the treatment of inner ear disorders (Figure 1) [14]. Indeed, this modality increased the native permeability of RWM *in-vivo* [15]. Several preclinical investigations described the reversible permeabilization of the outer epithelial layer of the RWM [16,17] in animal models, including guinea pigs [16,18–20]. Studies have reported the absence of ototoxic effects on cochlear function, thus demonstrating the safety of MB-assisted US [20,21]. The efficacy and the safety of this US modality are dependent on several key parameters including (i) the pathophysiological properties of the target tissues, (ii) the US parameters and device, (iii) the therapeutic scheme, and (iv) the pharmacological and physicochemical properties of therapeutic agents and MBs [22,23].

In this review, we focus on MBs, describing their formulation as well as their properties for *in-vitro* and *in-vivo* inner ear drug delivery. The different drug delivery strategies including the use of bare MBs (coadministration and sequential administration) and drug-loaded MBs are also compared. The limitations of the existing literature and future research directions are also discussed.

158

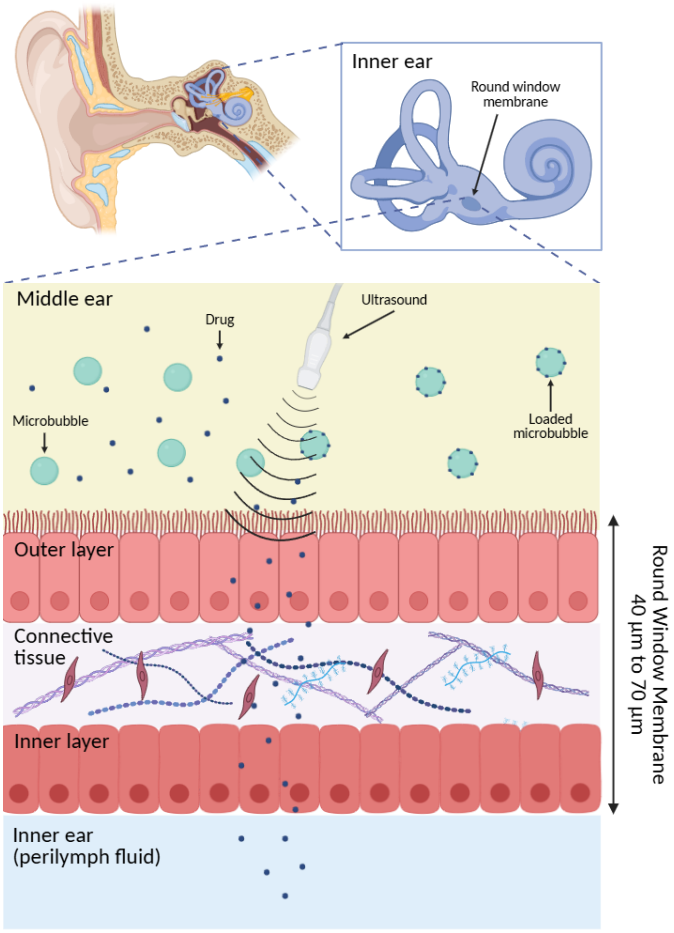

Figure 1: Principle of drug delivery using MB-assisted US through the round window membrane. Made with BioRender.

1. METHODS

Using the Preferred Reporting Items for Systematic Review and Meta-Analysis (PRISMA) recommended methods [24], MEDLINE (via PubMed®), the Cochrane Central Register of Controlled Trials (CENTRAL, via Wiley), and Web of Science™, electronic databases were screened using predefined search dates (January 1995 – January 2025) and specific terms for *in-vitro* and *in-vivo* drug delivery in the inner ear using MB-assisted US. The search terms used in these databases were ((loaded microbubbles) AND (inner ear)) OR ((charged microbubbles) AND (inner ear)) OR ((loaded microbubbles) AND (hearing loss)) OR ((charged microbubbles) AND (hearing loss)). An "English language" filter was applied. Table 1 summarizes the inclusion and exclusion criteria. The selection process began in November 2024 and was completed in March 2025. This process is outlined in Figure 2.

A formal risk-of-bias assessment was not performed in this review. The included studies consisted exclusively of heterogeneous preclinical *in-vitro* and *in-vivo* experiments, for which no validated and universally accepted risk-of-bias tools currently exist. The marked variability in experimental designs, biological models, US protocols, MB formulations, and outcome measures would limit the relevance and reliability of applying standardized assessment tools such as SYRCLE or ARRIVE-based metrics. For these reasons, and in line with several recent preclinical systematic reviews, we chose not to conduct a formal bias evaluation. This methodological limitation is acknowledged and addressed in the Discussion section.

Nineteen articles were analysed. After review, five articles were excluded because three did not concern MB-assisted US procedures, one was about nephrology, and one was a review. A total of fourteen articles were thus included in this review (Figure 2). Studies were performed *in-vitro* or on animals.

Table 1. Inclusion and exclusion criteria used to select studies

Inclusion criteria	**Exclusion criteria**
In-vitro, *In-vivo*	*In-silico*
Inner ear diseases	Not concerned with the inner ear
RWM opening and drug delivery	Drug delivery with US only or MBs only
English	Review papers, comments, and letters
MB-assisted US	Other languages

Abbreviations: MB: Microbubble; RWM: Round window membrane; US: Ultrasound.

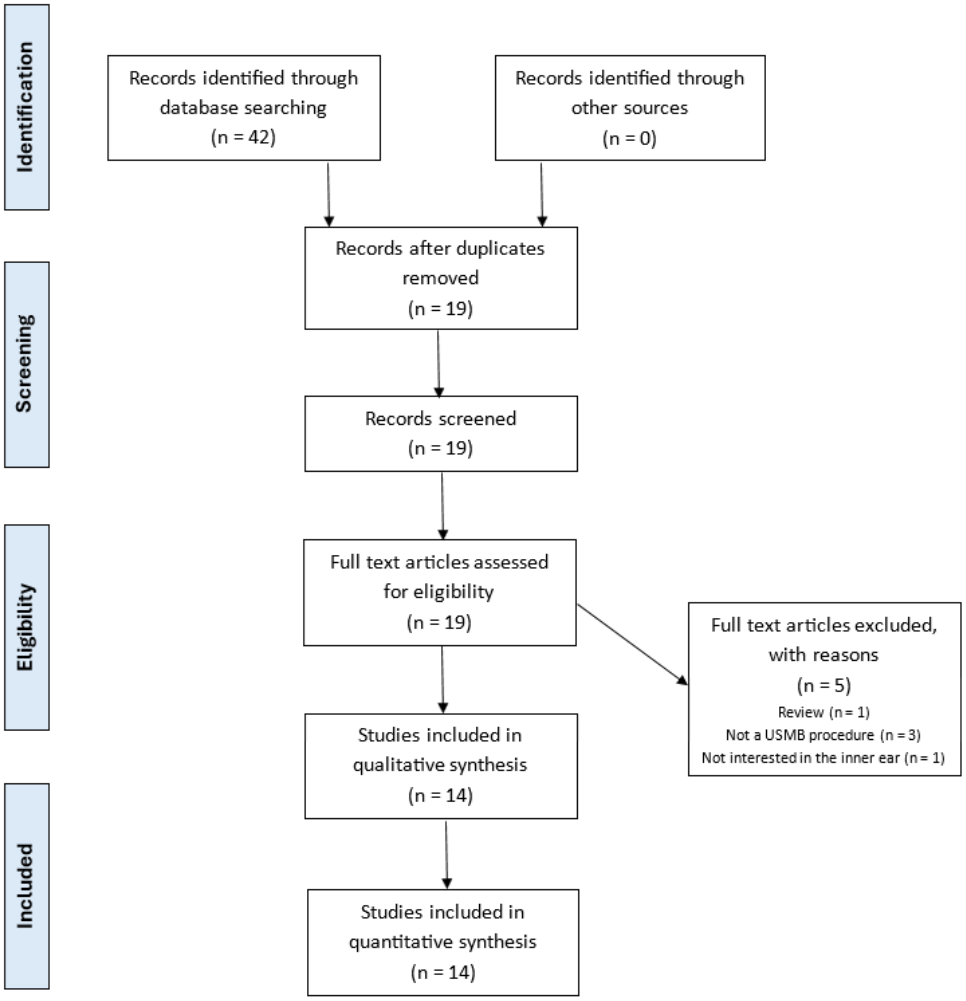

Figure 2: PRISMA Flow Diagram. The PRISMA diagram details the search and selection process applied during the review.

2. RESULTS

MBs are micrometer-sized colloidal particles (1–10 µm) with a thin biocompatible shell that encapsulates a gas core, suspended in an aqueous medium (Figure 3) [25]. MBs are commonly mixed with auditory cells for *in-vitro* studies or administered intravenously or locally for *in-vivo* inner ear drug delivery purposes. Their response to US stimulation depends on (i) acoustic parameters (*e.g.,* center frequency, acoustic pressure, pulse duration, *etc.*), (ii) physiological environment surrounding the MBs (*e.g.,* tissue perfusion, blood pressure, proximity of target cells/biological barriers, *etc.*), and (iii) the intrinsic properties of the MBs (*e.g.,* shell composition, gas, targeting, size, biocompatibility, compressibility, stability, *etc.*) and other MB-related parameters (*e.g.,* dose, administration route, pharmacokinetics, biodistribution, *etc.*). In this section, we review the physicochemical and pharmacological properties of MBs used for drug delivery in general and for inner ear drug delivery, specifically.

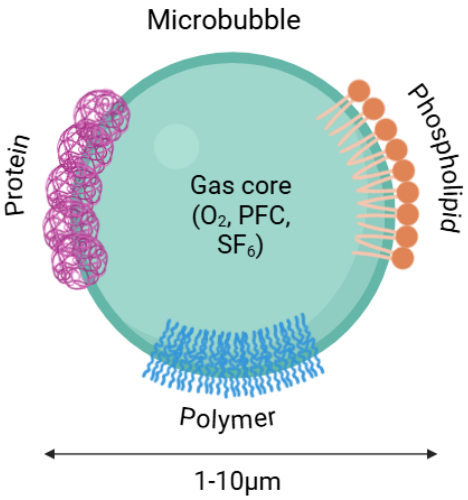

Figure 3: Scheme of microbubble. Made with BioRender.

3.1. General concepts of MBs

3.1.1. Gas

Historically, the early generations of MBs consisted of air core encapsulated by a biocompatible shell. However, these air-filled MBs dissolve in the bloodstream within seconds after intravenous injection due to the high solubility of air in blood and their limited resistance to arterial pressure gradients. To overcome these issues, a second generation of MBs was developed, which were filled with a single heavy-weight hydrophobic gas, including perfluorocarbon (*e.g.,* Definity® MBs), sulfur hexafluoride (SF_6; *e.g.,* SonoVue® MBs), or a mixture of gases such perfluorocarbon and nitrogen (*e.g.,* Vevo MicroMarker® MBs). SF_6-filled MBs are valued for their high compressibility and

low solubility in water, properties that contribute to their stability during US exposure. However, their relatively short half-life in blood—due to the faster dissolution of SF_6 in biological fluids compared to perfluorinated gases—limits their suitability for applications requiring prolonged US exposure [26]. In contrast, perfluorinated gases are characterized by higher density and lower solubility in blood, which slows gas diffusion between the MB core and the surrounding medium [27]. These properties result in a longer circulation time, making them particularly advantageous for sequential injection protocols, where there is a delay between MB administration and US exposure. Nevertheless, the increased density of perfluorinated gases may attenuate the acoustic response of the MBs, potentially reducing the efficiency of MB-assisted US. Currently, perfluorinated gases are preferred for the design of MBs for diagnostic and therapeutic applications; MBs containing therapeutic gases such as oxygen are also described for therapeutic applications in oncology [28].

The nature and quantity of gas in the MB core significantly influence the MB stability, their circulation persistence, the acoustic behavior, as well as their efficacy to permeabilize biological barriers and deliver therapeutic agents. The gas core of a MB is significantly more compressible (by several orders of magnitude) than an equivalent volume of blood. This high compressibility, combined with the low density of the core, creates a considerable impedance mismatch between the MBs and the surrounding medium, making them responsive to US.

3.1.2. MB shell

As mentioned above, MBs are gaseous bodies surrounded by a thin and biocompatible shell. This shell is approximately 5 to 200 nm thick. This thickness depends on the nature of the biocompatible elements that compose it. The shell of main commercial and clinically approved MBs, including SonoVue®, Definity® and Sonozoid® MBs, is made up of a lipid monolayer; differently. Optison® MBs utilize a human albumin shell [29–31]. The lab-made MBs are mainly lipid-shelled, but polymer- (*e.g.,* polylactic-co-glycolic) and protein-shelled MBs are also described [32]. The MB surface can be also functionalized with ligands and antibodies (*e.g.,* full size or fragments) to target receptors expressed (or overexpressed in pathophysiological context) on target cell membranes [33]. Such targeting agents are bound to the MB surface through electrostatic interactions or the use of pegylated shell components carrying conjugation agents such as thiol-maleimide, disulfide, or biotin [34]. The MBs can carry one or more targeting agents to increase their targeting specificity. Currently, targeted MBs are mainly designed as US contrast agents for US molecular imaging for the diagnosis and the characterization of cancers and inflammatory disorders. However, they may also be exploited for drug delivery purposes. Indeed, the targeted accumulation of these MBs on the cells or tissues ensures the precise, efficient and safe permeabilization of these targets, as well as the effective and secure delivery of therapeutic agents. Nevertheless, more preclinical and clinical investigations are required to provide relevant evidence of their use for drug delivery.

The primary role of the MB shell is to enhance the *in-vivo* MB stability by preventing MB coalescence, by increasing their resistance to arterial pressure gradients, and by reducing gas dissolution in the blood [35]. Thus, the circulation lifetime of MBs is often short-lived, typically 3-5 min for SonoVue® MBs. However, this lifetime can increase to tens of minutes depending on the composition of the MB shell (*e.g.,* PEGylated and polymeric MBs). The shell composition governs the

viscoelastic properties of MB shell, which strongly influence the acoustic behavior of MBs under US exposure. Indeed, lipid-shelled MBs are characterized by a thin and flexible shell ("soft-shelled MBs"), thus providing a great acoustic response [36]. On the contrary, the protein- and polymer-shelled MBs are defined as "hard-shelled MBs" because their shells are thicker and more rigid than those of lipid-shelled MBs. These properties provide hard-shelled MBs greater stability but only moderate acoustic behavior, compared to soft-shelled MBs under similar US conditions [37,38]. Consequently, adjustments in the chemical composition of shell and/or US parameters are required to improve the dynamic response of MBs under US exposure [39,40].

The charge surface of MBs plays a major role in imaging as well as therapeutic applications [41]. This parameter influences contrast enhancement, targeting efficiency, and circulation times by affecting the bulk interactions between the MBs and their environment (including proteins, cells and tissues). As recently reported [42,43], positively charged MBs showed a higher sensitivity and effectiveness in imaging applications than do neutral and negatively charged MBs, because of their stronger interactions with negatively charged biological targets (*e.g.,* endothelial cells or vascular structures). These interactions enhance MB retention at the imaging site, resulting in a stronger imaging signal that is useful for high resolution imaging [44]. As mentioned above, positively charged MBs are also relevant for therapeutic applications. Indeed, they can be carrier free or have complexed nucleic acids on their surface for gene delivery [45]. In contrast, negatively charged MBs are retained within capillaries via complement-mediated attachment to endothelium and thus exhibit longer circulation times than do neutral and positively charged MBs [46]. This property is exploited in imaging applications that require extended observation periods, in therapeutic applications for the repeated delivery of drugs in the target tissues, or in the delivery of long circulating drugs. Neutral MBs offer a balanced performance across all parameters [42]. For all these reasons, the commercially- and clinically-approved MBs, as well as lab-made MBs are mainly neutral or negatively charged.

3.1.3. MBs as drug vehicles

For the past 10 years, MBs have been also engineered to serve as drug carriers. As shown in Figure 4, lipophilic drugs can be embodied into the MB shell through hydrophobic interactions or dissolved in an oil cavity located between the gas core and the MB shell [47–49]. In addition, nucleic acids (*e.g.,* plasmid DNA, siRNA, miRNA, *etc.*) can be also loaded on surface of the cationic MBs through electrostatic interactions. While these strategies seem to be promising, the size of MBs and their gaseous lumen can restrict their drug loading capacity, thus not allowing the therapeutic dose to be reached [40]. The first approach to overcome such issue is the binding of drug-loaded nanoparticles (with hydrophilic or hydrophobic core as function of the nature of drug) or nucleic acid-packed nanocomplexes (with cationic lipids or polymers) on the MB surface through electrostatic or covalent interactions. In addition, the loading efficiency can be enhanced by applying multiple layers of these nanoparticles or nanocomplexes around the MB shell [50]. This approach may not be required for polymeric MBs because several studies reported that significant quantity of drugs (more specifically for hydrophobic rather than hydrophilic drugs) can be loaded into their shells. Some studies have explored the potential of loading MB with viral vectors with for gene therapy purposes [51]. The

administration of high doses of drug-loaded MBs or their repeated administration also constitute two other technical alternatives to achieve therapeutic doses. These options are discussed further below.

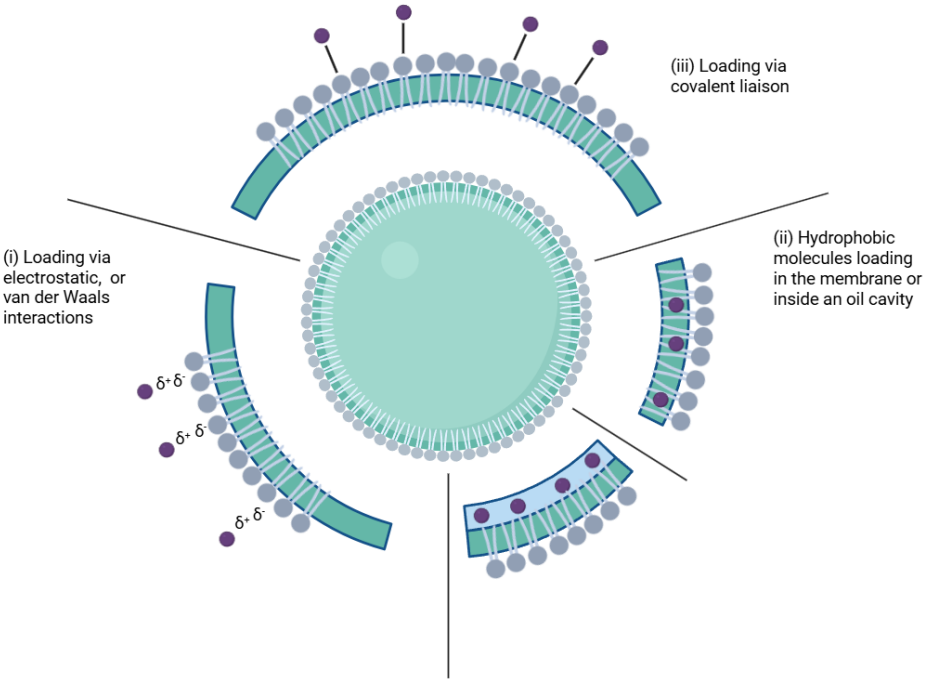

Figure 4: Schematic representation of the various options for the design of drug loaded microbubble. Made with BioRender.

Drug-loaded MBs offer several advantages over bare MBs. Drug-loaded MBs protect the drug against its degradation and clearance, thus enhancing its circulation lifetime and minimizing adverse effects on healthy tissues. In addition, drug-loaded MBs can release the drug in a controlled and specific manner into the target cells or tissues under the effect of US stimulation, ensuring that both the MBs and drug will be in contact with the target cells and tissues at the same time when the US is applied, thus maximizing the chances of effective drug delivery. However, loading drugs into MBs can alter the pharmacological properties of the drugs (*e.g.,* pharmacokinetics, biodistribution, pharmacodynamics) as well as the acoustic properties of the MBs. Therefore, further studies are needed to investigate these potential effects. Currently, drug-loaded MBs are mainly investigated in preclinical studies for the treatment of cancers, cardiovascular and brain disorders [52]. These MBs represent new therapeutic entities, which require extensive and expensive testing to evaluate their safety and efficacy for their clinical approval.

3.1.4. MB size

The original development of MBs was to provide image contrast while remaining safe for intravenous injection by restricting their size to be < 10 µm [53]. Thus, the average diameter is 2.5 µm for clinically approved and most lab-made MBs, though their diameter can range from 1 to 10 µm.

They also show a very broad polydispersity in size. Because to their micrometer size range, MBs are restricted to the vasculature and pass through the pulmonary system after a standard intravenous injection (*i.e.,* bolus or infusion). They serve as pure intravascular tracers for imaging purposes, as well as therapeutic MBs for systemic drug delivery [54].

Drug delivery using MB-assisted US requires that MBs be present in close contact with the target cells or tissues to increase their permeability, albeit reversibly [55]. This permeabilization does not occur in the absence of MBs, making the MBs a key component of this modality. As discussed above, US-induced volumetric oscillations of MBs play a major role in the reversible permeabilization of biological barriers. Several *in-silico* and *in-vitro* investigations reported that the oscillation amplitude of MBs, their resonance frequency, their pressure threshold for cavitation (*e.g.,* stable or inertial), their translational velocity, the lifetime of MB oscillation all depend on the environment surrounding the MBs as well as the size of the MBs [56–60]. While MBs must remain within the micrometer range for safety during i.v. administration, recent evidence highlights that monodisperse MBs respond more uniformly to US, as all MBs in the population share a similar resonance frequency. In contrast, only a fraction of a polydisperse MB population will resonate effectively at a given frequency and pressure [61]. This has direct implications for acoustically mediated drug delivery: polydispersity reduces the overall efficiency of barrier permeabilization and intracellular uptake, as shown in multiple *in-vitro* and *in-vivo* studies [62–64]. Furthermore, MB size heterogeneity affects drug loading and release behavior. Larger MBs generally offer greater surface area and shell volume for drug loading, whereas smaller MBs may load significantly less drug and undergo faster destruction under US. As a result, polydisperse formulations can lead to heterogeneous loading efficiencies and unpredictable release kinetics. Monodisperse MBs, which can be produced with microfluidic technologies, provide more consistent oscillation patterns and thus more reproducible and controllable drug delivery profiles. However, these monodisperse formulations are not yet clinically approved.

3.1.5. Administration route and mode

For *in-vitro* experiments*,* a monolayer of adherent cells or a suspension of cells are incubated with a mixture of MBs and the therapeutic agents or drug-loaded MBs [65,66]. Then, US waves are immediately applied. For *in-vitro* experiments, MB concentrations commonly range from 10^2 to 10^4 MBs/mL. In the case of separate administration, MBs and therapeutic agents can be handled entirely independently prior to their co-incubation with cells. In contrast, drug-loaded MBs are directly incubated with cells as a single formulation. Notably, while the concentration and volume of MBs and therapeutic agents can be independently adjusted in the former approach, they are inherently interdependent in the latter. More recently, MB-assisted US have also used to deliver therapeutic agents in tumor spheroids and organoids [67,68].

In-vivo, intravenous administration of MBs is most commonly used, providing access to superficial and deep-seated tissues [69,70]. Variable concentrations of MBs, ranging from 10^4 to 10^{10} MBs/mL, can be injected intravenously. However, the choice of MB concentration is often empirical and poorly explained in *in-vivo* studies [18,71]. The intravenous route is a relatively easy and safe way for injection of MBs as well as therapeutic agents in a clinical setting. The main limitations of this route

are: (i) the short circulation time of MBs, which need to be sufficiently accumulated in the vasculature of the targeted tissues and exposed to US within minutes after intravenous injection, and (ii) the rapid plasma clearance of therapeutic agents and their unspecific accumulation in healthy tissues. As previously discussed, the formulation of MBs and drugs can be optimized to overcome these shortcomings. It is important to note that the success of acoustically mediated drug delivery through intravenous administration of MBs and therapeutic agents relies on the sufficient vascularization of the targeted tissues. By using the intravenous route, the MBs and the therapeutic agents can either be co-administered or administered sequentially (*i.e.,* an intravenous injection of MBs followed by another injection of the therapeutic agents, or vice versa). The choice between administration modalities depends on the physicochemical and pharmacological properties of the therapeutic agents. Both offer the advantage that clinically approved MBs and therapeutic agents can be delivered directly in humans without additional approval from health authorities, compared to drug-loaded MBs [72–74]. In addition, they can be handled completely independently until their injection, unlike drug-loaded MBs.

Local administration routes, such as intratissue or intracavitary injection, represent the most direct approach for delivering therapeutic agents [20,75,76]. A wide range of MB concentrations, typically spanning from 10^4 to 10^6 MBs/mL, has been reported for local injection. Compared to systemic administration, this strategy offers several advantages, including the circumvention of the transendothelial barrier and the generation of transient interstitial pressure gradients. It enables the localized delivery of high concentrations of therapeutic agents to the target tissue while minimizing systemic exposure and off-target effects. Additionally, local injection can overcome challenges related to the short plasma half-life of therapeutic agents and MBs observed with intravenous administration. Once injected within the tissue, therapeutic agents and MBs are distributed within via diffusion and convection, and subsequent US exposure enhances cellular uptake [77]. Despite its benefits, this route is limited by factors such as the permissible injection volume and the accessibility of the target tissue, thereby confining its application mainly to superficial tissues or accessible through a natural cavity or surgery. It is important to note that most technical data available on MB stability, cavitation, and pharmacokinetic behavior originate from studies performed in blood, which differs markedly from perilymph and may therefore not fully predict MB behavior in the inner ear.

3.2. Applications to the inner ear

In this section, we focus on MB formulations (*i.e.,* gas core, shell composition, *etc.*) and MB-related parameters (*i.e.,* concentration, route and mode of administration, *etc.*) used for the delivery of therapeutic agents using MB-assisted US in *in-vitro* and *in-vivo* settings applied to the inner ear model.

3.2.1. *In-vitro* drug delivery

To date, only six publications have reported on the design and/or evaluation of MBs for *in-vitro* acoustically mediated delivery of therapeutic agents (*e.g.,* Cy3 siNOX4; IGF-1; DEX), or of molecules mimicking these agents (*e.g.,* Biotin-FITC; pEGFP-C1; FITC-CS-AuNPs); see Table 2. The main *in-vitro* models employed in these studies include HEI-OC1 auditory hair cells for nucleic acid

Table 2. Characteristics of MBs used in *in-vitro* sonoporation studies (n=6)

Reference	Drug	*In-vitro* model	MBs name	Shell composition	Gas Type	Surface charge	Diameter (µm)	Concentration (MBs/mL)	Volume (mL)
Lin *et al.*, (2024) [78]	Cy3 siNOX4	HEI-OC cells	Lysozyme-shelled	Lysozyme	C_3F_8	Positive	2.66 ± 0.04 to 4.01 ± 0.26	2.4 x 10^7, 1.2 x 10^7, or 0.6 x 10^7	NA
Liao *et al.*, (2022) [79]	IGF-1	Static Franz diffusion cells	Albumin-shelled	Albumin	C_3F_8	Negative	1.06 ± 0.04 to 3.01 ± 0.06	1.2 x 10^7	1
Liao *et al.*, (2021) [21]	Dexamethasone + P407 + Biotin-FITC	Static Franz diffusion cells	Albumin-shelled	Albumin	C_3F_8	Negative	2.70 ± 0.17	4.2 x 10^7	NA
Lin *et al.*, (2021) [19]	FITC-CS-AuNPs	HEI-OC1 cells	SonoVue®	DSPC/DPPG/PA	SF_6	Negative	1.90	2 x 10^8	NA
Liao *et al.*, (2020) [80]	Biotin-FITC	3D printed diffusion device	Albumin-shelled	Albumin	C_3F_8	Negative	1.02 ± 0.11	1.4 x 10^7	0.5
Liao *et al.*, (2014) [81]	pEGFP-C1	HEI-OC1 cells	Albumin-shelled	Albumin/ dextrose	C_3F_8	Negative	0.66 ± 0.02 to 3.47 ± 0.53	2 × 10^8	NA

Abbreviations: Cy3 siNOX4: cellular uptake of cyanine 3 small interfering NADPH oxidase-4; IGF-1: Insulin-like growth factor-1; C_3F_8: Perfluoropropane; P407: Poloxoamer 407; DSPC: Di-Stearoyl-Phosphatidyl-Choline; DPPG: Di-palmitoyl-phosphoglycerol; PA: Palmitic Acid; SF6: Sulfur hexafluoride; NA: Not available.

Commenté [JE1]: Je ne sais pas pourquoi mais le tableau est au milieu du texte

transfection [19,78,81], as well as static Franz diffusion cells [21,79] and lab-printed diffusion systems to study RWM permeabilization and therapeutic agent delivery [80].

Among these six *in-vitro* studies, four used lab-manufactured albumin-shelled MBs [21,79–81], one used clinically approved phospholipid-shelled MBs (SonoVue®) [19], and one used Lysozyme-shelled MBs [78]. Albumin-shelled MBs and Lysozyme-shelled MBs possess a gaseous core composed of perfluoropropane, whereas SonoVue® MBs contain sulfur hexafluoride gas. The Albumin- and Lysozyme-shelled MBs typically range in diameter from ~ 0.5 to 3.5 µm, while the SonoVue® MBs exhibit a mean diameter of ~ 2 µm. All the MBs are characterized by size polydispersity. The albumin-shelled and SonoVue® MBs exhibit a negatively charged surface, whereas the Lysozyme-shelled MBs have a positively charged surface. The final concentrations range from 1×10^7 to 2×10^9 MBs/mL for Albumin-shelled MBs, and from 0.6×10^7 to 2.4×10^7 MBs/mL for Lysozyme-shelled MBs; the final concentration for SonoVue® MBs range is 2×10^8 MBs/mL. Among the six *in-vitro* studies reviewed, MBs were co-administered with therapeutic agents in two studies [21,80] and administered sequentially in another two studies [19,81]. Two other studies investigated drug-loaded MBs [78,79].

The albumin-shelled MBs have proven to be particularly effective for transfecting HEI-OC1 cells and for delivering FITC-Biotin, DEX, and IGF-1 *in-vitro*. Liao *et al.* [81] investigated the effects of shell composition (specifically, the presence or absence of dextrose in the MB shell) and size (with diameter ranging from 0.5 to 3.5 µm) on the transfection efficiency of HEI-OC1 cells. As previously discussed, the presence of dextrose in the shell of these MBs alters their physicochemical, pharmacological, and acoustic properties (*e.g.,* producing a thinner shell, improved *in-vivo* stability, and a broader range of resonance frequency), thereby influencing the *in-vitro* transfection efficiency. The authors demonstrated first that the diameter of the MBs increased with the proportion of albumin or dextrose in the MB shell. Thus, MBs with diameters between 3 and 3.5 µm (considered to be larger MBs by the authors) exhibited either a higher dextrose concentration and lower albumin concentration, or a higher albumin concentration. These larger MBs led to transfection rates of 80 to 85%, regardless of MB formulation. For smaller MBs (*i.e.,* with a diameter of ≤ 2 µm), albumin-shelled MBs containing dextrose were half as effective at transfecting cells compared to standard albumin-

shelled MBs. In addition, the transfection efficiency increased with MB diameter regardless of the MB formulation. To understand the relationship between MB size and transfection efficiency, the acoustic behavior of MBs was investigated. Surprisingly, the efficiency of MB destruction was inversely proportional to MB size. These results can be explained by the fact that the acoustic behavior of MBs depends not only on the US parameters but also on the physicochemical properties and the size of the MBs. With application of US, smaller MBs were readily destroyed, suggesting that they may become unstable and fragment before interacting with cells. Conversely, the stable cavitation of larger MBs in close proximity to the cell membrane during their lifespan may enhance membrane permeabilization, thus facilitating intracellular delivery of plasmid DNA without affecting cell viability. In conclusion, MB-assisted US using albumin-shelled MBs is an effective and safe modality for cell transfection.

In Liao *et al.* [81], MBs were first incubated with the cells to induce membrane permeabilization following US exposure. Subsequently, pDNA lipoplexes were added to the cells. However, these cationic lipoplexes could have been directly loaded onto the negatively charged surface of these MBs prior to incubation with the cells and US application. An alternative approach could have involved leveraging the physicochemical properties of albumin-shelled MBs, which are capable of incorporating large quantities of pDNA within their thick shell—unlike phospholipid-shelled MBs [40]—or employing cationic MBs that allow for direct pDNA loading through electrostatic interactions [82]. Liao *et al.* [79] took advantage of the negative surface charge of albumin-shelled MBs to load human insulin-like growth factor 1 (IGF-1), which contains seven positively charged amino acid residues. IGF-1 is regarded as a promising novel therapeutic agent for treatment of SNHL and has been investigated in clinical trials involving patients with idiopathic sudden SNHL, who are refractory to systemic steroid therapy. The concentration of the IGF-1 loaded MBs (12×10^8 MBs/mL) did not correlate with the albumin concentration. However, both the size (ranging from 1 to 3 µm in diameter) and the surface charge (ranging from −14 to −25 mV in zeta potential) of the MBs increased with the composition ratio of albumin. The IGF-1 loading efficiency onto the MB surface (ranging from 58% to 71%) increased with MB size. This loading altered the surface charge of the loaded MBs, making it more positive compared to unloaded MBs. No information was provided regarding the impact of IGF-1 loading on MB size. *In-vitro* acoustically mediated delivery of IGF-1 across the RWM was investigated using albumin-shelled MBs of varying diameters (1 to 3 µm; 1.2×10^7 MBs/mL) in combination with a Franz diffusion cell system. Independent of MB size, the exposure of this system to US resulted in a significant 3-fold increase in IGF-1 penetration and release compared to treatment with IGF1-loaded MBs alone, in the absence of US. Among the different sizes tested, IGF1-loaded MBs measuring 3 µm in diameter exhibited superior performance in facilitating IGF-1 penetration and release. Taken together, these findings suggest that MB-assisted US using IGF-1–loaded MBs appears to be a promising strategy for the treatment of hearing disorders.

Lin *et al.* [78] compared the co-administration approach to the use of loaded MBs for delivery of small interfering RNA that targeted the messenger RNA of nicotinamide adenine dinucleotide phosphate oxidase 4 (siNOX4), a key player in cisplatin-induced ototoxicity for cochlear hair cells [78]. To this end, lysozyme-shelled MBs were engineered for the co-delivery of naked siNOX4 and for the encapsulation of siNOX4 (siNOX4 loaded MBs). As previously discussed, positively charged MBs

enable the efficient loading of negatively charged therapeutic nucleic acids. Both strategies were evaluated for their ability to deliver siNOX4 *in-vitro* to HEI-OC1 cells and *ex-vivo* in mouse organ of Corti explants. Exposure of cisplatin-treated HEI-OC1 cells to siNOX4-loaded MBs in the presence of US resulted in a higher transfection efficiency compared to the co-administration approach (25% *vs* 19%). The acoustically mediated delivery of siNOX4 in cisplatin-treated organ of Corti explant cultures using siNOX4-loaded MBs led to a significant reduction in NOX4 expression, thereby mitigating ototoxicity. In conclusion, the study demonstrated the superiority of the loaded MB approach over the co-administration approach for the treatment of auditory disorders.

Taken together, the *in-vitro* studies demonstrate that MB-assisted US represents a promising strategy to deliver a broad range of therapeutic agents aimed at treating hearing disorders. The MB size and their shell composition were the primary parameters that were evaluated *in-vitro*. Notably, the effects of MB concentration, their size polydispersity, and their gas core composition have not been systematically investigated in the delivery of therapeutic agents, despite the relative ease of conducting such *in-vitro* studies. Furthermore, no *in-vitro* comparative studies have been conducted to assess the efficacy of soft-based versus hard-shelled MBs, or to evaluate differences between co-administration of MBs with therapeutic agents versus pre-loaded MBs with the same agents.

3.2.2. *In-vivo* drug delivery

To date, twelve preclinical studies have investigated *in-vivo* acoustically mediated delivery of either marker agents [*e.g.,* Biotin-FITC; rAAV; FITC-CS-AuNPs; Fe_3O_4; CUR) to evaluate RWM permeabilization, or to deliver the therapeutic agents [*e.g.,* IGF-1; DEX; gentamicin] for the treatment of hearing disorders; see Table 3. The primary animal models employed included mice [19], guinea pigs [14,16–18,21,71,79,80,83,84], and sheep [20].

Among these preclinical studies, seven used phospholipid-shelled MBs [16,17,19,20,71,83,84] including clinically approved formulations such as SonoVue® [17,19,71,84], Definity® MBs [16], and Vevo MicroMarker® MBs [20], which are commercially available for preclinical US imaging. The remaining studies used laboratory-produced albumin-shelled MBs [14,18,21,71,79,80]. Albumin-shelled and Definity® MBs possess a gaseous core composed of perfluorocarbone gas, whereas SonoVue® and Vevo MicroMarkers® MBs contain sulfur hexafluoride gas and a mixture of perfluorobutane and nitrogen gases, respectively. The albumin-shelled and Definity® MBs typically range in diameter from ~ 1 to 3 µm, while the mean diameter is ~ 2 µm for SonoVue® MBs and ~2.5 µm for Vevo MicroMarker® MBs. In these preclinical studies, all MBs were characterized by their micrometer-scale size, a high degree of size polydispersity, and a negatively charged surface. The final concentrations ranged from 1×10^7 to 4×10^9 MBs/mL for Albumin-shelled MBs and 1.2×10^{10} MBs/mL the Definity® MBs, versus 2×10^8 MBs/mL for the SonoVue® and Vevo MicroMarker® MBs. The high concentrations of MBs used in some of these studies [14,16,18] were striking , compared to those used for common applications of MB-assisted US such as neurology, oncology, and cardiology. The elevated concentrations were all the more surprising given that, in most cases, MBs were administered locally. While MB concentration has been positively correlated with enhanced cell and tissue permeabilization [85,86], excessively high concentrations may, conversely, hinder US propagation and limit tissue permeabilization. To our knowledge, no *in-vivo* study to date has specifically investigated the effect of MB concentration on

the permeabilization of the RWM. Among delivery strategies, co-administration was the most commonly used [14,18,21,71,80,83], followed by sequential administration [16,17,19,84], and drug-loaded MB approaches [79]. Notably, one preclinical study did not deliver any therapeutic agent, focusing instead on assessing the safety of US-mediated RWM permeabilization [20]. Only one study investigated drug-loaded MBs. Regarding the route of administration, nearly all studies employed local delivery of MBs and therapeutic agents: nine via the retroauricular route and two via transtympanic injection. Only one study investigated co-administration via the intravenous route to investigate therapeutic delivery to the inner ear [83].

Table 3. Characteristics of MBs used in *in-vivo* sonoporation studies (n=12)

Reference	Drug	MBs type	Shell composition	Gas type	Surface Charge	Diameter (µm)	Concentration (MBs/mL)	Volume (mL)	Route of administration
He *et al.*, (2024) [83]	Fe_3O_4 or CUR or DSP	PEG-shelled	DSPC/DSPE-PEG2000	SF_6	Negative	1.50 ± 0.50	1.44×10^6	0.5 mL/kg	IV
Kerneis *et al.*, (2023) [20]	No drug	Vevo MicroMarker™	PEG/ Phospholipids	C_4F_{10}/ N_2	Negative	2.30 - 2.90	2×10^8	0.9	Middle ear cavity
Liao *et al.*, (2022) [79]	IGF-1	Albumin-shelled	Albumin	C_3F_8	Negative	1.06 ± 0.04 to 3.01 ± 0.06	1.2×10^7	NA	Middle ear cavity
Liao *et al.*, (2021) [21]	Dexamethasone-P407	Albumin-shelled	Albumin	C_3F_8	Negative	2.70 ± 0.17	4.2×10^7	0.2	ITT
Lin *et al.*, (2021) [19]	CSAuNPS	SonoVue®	DSPC/DPPG/ PA	SF_6	Negative	1.90	$2\text{-}5 \times 10^8$*	0.5 - 0.6	Middle ear cavity
Lin *et al.*, (2021) [84]	IGF-1	SonoVue®	DSPC/DPPG/ PA	SF_6	Negative	1.90	$2\text{-}5 \times 10^8$*	0.2	Middle ear cavity
Liao *et al.*, (2020) [80]	Gentamicin	Albumin-shelled	Albumin	PFC	Negative	1.02 ± 0.11	1.4×10^7	0.2	ITT
Lin *et al.*, (2020) [17]	Biotin-FITC	SonoVue®	DSPC/DPPG/ PA	SF_6	Negative	1.90	$2\text{-}5 \times 10^8$*	0.2	Middle ear cavity
Zhang *et al.*, (2020) [16]	AAV2/Anc80L65	Definity®	DPPC/DPPA/ 5000-DPPE	C_3F_8	Negative	1.10 – 3.30	1.2×10^{10}*	NA	Middle ear cavity
Shih *et al.*, (2019) [71]	Dexamethasone	SonoVue® or Albumin-shelled	DSPC/DPPG/ PA or Albumin	SF_6 or C_3F_8	Negative	1.90 or 7.09	$2\text{-}5 \times 10^8$ or 2.9×10^8	0.2	Middle ear cavity
Shih *et al.*, (2013) [18]	Biotin-FITC or gentamicin	Albumin-shelled	Albumin	PFC	Negative	NA	4×10^9	0.2	Middle ear cavity
Liao *et al.*, (2012) [14]	Biotin-FITC	Albumin-shelled	Albumin	PFC	Negative	NA	4×10^9	0.2	Middle ear cavity

Abbreviations: Fe_3O_4: Iron oxide III; CUR: Curcumin; DSP: Dexamethasone Sodium Phosphate; DSPC: Di-Stearoyl-Phosphatidyl-Choline; DSPE-PEG 2000: Di-Stearoyl-Phosphoryl-Ethanolamine-PolyEthylene Glycol 2000; SF_6: Sulfur hexafluoride; IV: Intravenous; PEG: PolyEthylene glycol; C_4F_{10}: Perfluorobutane; N_2: Nitrogen; IGF-1: Insulin-like growth factor-1; C_3F_8: Perfluoropropane; P407: Poloxamer 407; ITT: Injection Trans-Tympanique; CS-AuNPs: Nano-chitosan capped gold nanoparticles; DPPG: Di-Palmitoyl-PhosphoGlycerol; PA: Palmitic Acid; PFC: Perfluorocarbon; Biotin-FITC: Fluorescein IsoThioCyanate conjugated biotin; DPPC: Di-Palmitoyl-Phosphatidyl-Choline; DPPA: Di-Palmitoyl-Phosphoric Acid; 5000-DPPE : 500-Di-Palmitoyl-Phosphatidyl-Ethanolamine; HSA: Human Serum Albumin; NA : Non-available

* Stock solution

Shih *et al.* [71] investigated the efficacy of US-mediated trans-RWM delivery of DEX using both SonoVue® and albumin-shelled MBs, as well as its preventive effects against noise-induced hearing loss in animal models. DEX, a glucocorticoid, is widely used in the treatment of hearing disorders such as SNHL, acoustic trauma, and Ménière's disease. Therapeutic efficacy strongly depends on achieving sufficient concentrations in the perilymph. To enhance perilymphatic DEX concentration, the authors filled the tympanic bulla of guinea pigs with a mixture of DEX and MBs, followed by US exposure. Two hours later, the animals were subjected to white noise exposure. Compared to passive diffusion, DEX delivery was enhanced by ~ 3.0- to 11.2-fold using SonoVue® MBs and by 2.4- to 7.9-fold with albumin-shelled MBs. Based on these results, the authors selected SonoVue® MBs to further evaluate

therapeutic efficacy. Their findings demonstrated that US-mediated DEX delivery provided significant cochlear protection and attenuated noise-induced hearing loss. The study underscored the importance of comparing different MB formulations to identify the most effective carrier for therapeutic delivery.

Liao *et al.* [79] designed therapeutic MBs loaded with recombinant IGF-1 protein and confirmed their ability to deliver IGF-1 across the RWM using a Franz diffusion cell system. They further evaluated the *in-vivo* efficacy of their strategy by introducing IGF-1-loaded MBs into the middle ear cavity, positioning an US transducer on the bony fenestration of the tympanic bulla, and exposing the target region to US. Two hours post-treatment, lymphatic fluid was collected to quantify IGF-1 concentration. The MB-assisted US resulted in a 16-fold increase in IGF-1 levels compared to control conditions. Immunohistochemical analysis of IGF-1 biodistribution revealed a markedly enhanced presence of IGF-1 in the basal, second, and third turns of the cochlea relative to controls. Additionally, this strategy facilitated significant IGF-1 distribution in regions containing inner hair cells. Histopathological evaluation and auditory brainstem response (ABR) recordings demonstrated that MB-assisted US caused no detectable structural or functional damage to the inner ear. The study demonstrated the efficacy and safety of acoustically mediated IGF-1 delivery using IGF-1–loaded MBs, although the therapeutic benefit of this strategy was not assessed.

Surprisingly, He *et al.* [83] opted for intravenous administration of both laboratory-made MBs and therapeutic agents, whereas all other preclinical studies employed local administration routes (*i.e.,* retroauricular or transtympanic injection). Specifically, they aimed to transiently permeabilize the blood–labyrinth barrier using MB-assisted US in order to deliver DEX and curcumin (CUR) in a guinea pig model of cisplatin-induced ototoxicity. MBs with either dexamethasone (DEX) or curcumin (CUR) were co-administered intravenously, followed by US exposure of the auditory canals. One-hour post-treatment, perilymph samples were collected, and the concentrations of DEX and CUR were quantified using high-performance liquid chromatography system coupled with spectrophotometer. The MB-assisted US resulted in a 2-fold increase in DEX and CUR concentrations in the perilymph compared to administration of DEX and CUR without US. ABR and immunohistological analyses were subsequently conducted to assess the protective effects of DEX and CUR against cisplatin-induced ototoxicity. Acoustically mediated delivery of DEX and CUR resulted in significantly better preservation of hearing, with ABR thresholds of 60 dB and 70 dB respectively, compared to higher thresholds observed following administration of DEX (75 dB) and CUR (90 dB) alone, or no treatment (105 dB). Immunohistological evaluation of the cochlear membrane further confirmed these findings by demonstrating improved integrity of outer hair cells. Collectively, these results demonstrate that MB-assisted US is an effective strategy for delivering both hydrophobic (DEX) and hydrophilic (CUR) agents to the inner ear via intravenous administration.

In conclusion, the preclinical *in-vivo* findings corroborate the *in-vitro* results and clearly demonstrate that MB-assisted US represents a potent and effective modality for targeted delivery of therapeutic agents in the treatment of hearing disorders. While both *in-vitro* and *in-vivo* studies have clearly demonstrated that US enables the delivery of a wide range of therapeutic agents—including corticosteroids, antibiotics, nucleic acids, recombinant proteins, and viral vectors for gene therapy—very few have systematically investigated and compared the physicochemical (*e.g.,* shell composition,

gas core, surface charge, size, concentration, *etc.*) and pharmacological (*e.g.,* pharmacokinetics, biodistribution, *etc.*) properties of MBs. Furthermore, no *in-vivo* comparative investigations have been conducted to evaluate the differences between co-administration or sequential administration of MBs with therapeutic agents, and the use of drug-loaded MBs carrying the same agents, nor to systematically assess the impact of different administration routes on delivery efficiency and therapeutic outcomes.

4. DISCUSSION

Targeted delivery of therapeutic agents using MB-assisted US holds significant promise as a clinically viable strategy for enhancing local therapies in otology. An increasing number of *in-vitro* and preclinical studies have demonstrated the effectiveness of MB-assisted US in facilitating the delivery of therapeutic agents, as well as the therapeutic benefits of this approach in various experimental models of hearing disorders.

However, direct comparison of outcomes across these studies is challenging due to substantial heterogeneity in MB formulations, including variations in their physicochemical and pharmacological properties, and the absence of standardized MB-related parameters (*e.g.,* concentration, route of administration, *etc.*). Notably, clinically approved MBs such as SonoVue® and Definity® have been utilized in only 36% of existing studies [16,17,19,71,84], despite their potential relevance for facilitating clinical translation of this US modality. Note that these MBs were originally developed for diagnostic US imaging and have not been specifically optimized for drug delivery applications [54]. Moreover, any adverse effects observed during therapeutic protocols may compromise future diagnostic use of these clinically approved MBs. This consideration partly explains why more than half of recent *in-vitro* and preclinical studies used lab-made MBs [14,18,21,71,78–81,83]. Lab-made MBs are specifically formulated to enable control over a broad range of physicochemical and pharmacological parameters and are intended to be optimized for drug delivery purposes. The typical profile of the most commonly used lab-made MBs consists of a gaseous perfluorocarbon core encapsulated by a biocompatible albumin shell. These MBs generally carry a negative surface charge, exhibit polydispersity in size, and have a mean diameter ranging from 1 to 3 µm. However, translating these lab-made MBs to clinical use would require extensive and costly characterization and validation to meet regulatory and health authority standards, thereby delaying their clinical application in therapeutic settings. It is important to note that none of the reviewed studies have employed targeted MBs. However, recent advances in inner ear drug delivery have introduced other classes of targeted or engineered carriers, such as hollow mesoporous silica@ZIF capsules for local gentamicin delivery [87] and metal–organic framework-based systems designed for the treatment of noise-induced hearing loss [88]. Although these nanocarriers do not rely on MB-assisted US, they illustrate the diversity of emerging strategies for improving cochlear drug targeting and highlight the need to position MB-based approaches within this broader landscape. With regard to US protocols, the majority of studies applied a single set of MB-related parameters to demonstrate therapeutic efficacy. These protocols often lack clarification on whether the parameters were selected based on systematic optimization or derived empirically from existing literature. Furthermore, only a limited number of studies have rigorously investigated and compared the physicochemical (*e.g.,* shell composition, gas core, surface charge, size,

concentration, *etc.*) and pharmacological (*e.g.,* pharmacokinetics, biodistribution, *etc.*) properties of MBs [71,79–81]. While the former approach is more suitable for optimizing the safety and efficacy of US protocols, it is associated with high costs and may raise ethical concerns related to the extensive use of animal models required for such comprehensive investigations. Although the physicochemical, acoustic, and pharmacokinetic properties of MBs are well characterized in blood, no study has yet evaluated these parameters in perilymphatic fluid. Because perilymph differs substantially from blood in viscosity, protein concentration, ionic composition, and passive diffusion dynamics, MB behavior in this compartment may deviate from what has been described in the systemic circulation. As a result, the mechanistic insights derived from blood-based investigations cannot be directly extrapolated to the inner ear environment. This constitutes an important limitation of the current literature and highlights the need for dedicated biophysical studies to characterize MB dynamics within inner ear fluids. This extensive heterogeneity also prevented the application of any standardized risk-of-bias framework, as no validated tool is appropriate for such diverse preclinical *in-vitro* and *in-vivo* studies; this constitutes an inherent methodological limitation of our review.

Beyond differences in formulation, the intrinsic physicochemical properties of MBs—particularly their size distribution, shell composition, and surface charge—play a decisive role in shaping US-mediated effects and may partly explain the variability observed across studies. MB size governs resonance frequency, cavitation thresholds, oscillation amplitude, and destruction dynamics; polydisperse formulations inevitably lead to heterogeneous oscillation behaviors, reducing the reproducibility and efficiency of RWM permeabilization. Monodisperse MBs, although not yet clinically approved, offer more predictable cavitation profiles and could improve the consistency of drug delivery outcomes. Likewise, shell viscoelasticity critically influences MB stability and acoustic responsiveness: soft lipid-shelled MBs generally exhibit stronger oscillations and higher permeabilization potential, whereas stiffer protein- or polymer-shelled MBs provide greater stability but attenuated cavitation activity. Finally, surface charge affects interactions with biological barriers, drug loading efficiency for nucleic acid delivery, and biodistribution. Together, these parameters strongly modulate therapeutic performance and highlight the need for systematic optimization of MB design in the context of inner ear drug delivery.

Furthermore, co-administration or sequential administration of MBs and therapeutic agents has been employed in ~ 85% of recent studies [14,16–21,71,80,81,83,84]. This strategy appears to be the most promising for clinical translation, particularly when it involves the use of clinically approved therapeutic agents and MBs. It also offers the advantage of independently adjusting the concentration and volume of each compound prior to *in-vitro* incubation or *in-vivo* administration. However, the success of acoustically mediated drug delivery using this approach relies heavily on the sufficient accumulation of both components at the biological target site. Due to differences in their physicochemical properties, MBs and therapeutic agents do not necessarily exhibit similar pharmacokinetics and biodistribution profiles. To address this limitation, drug-loaded MBs have been developed, enabling the co-localization of both agents at the target site and facilitating localized drug release upon US exposure. Despite their potential, this approach has been explored in only 15% of existing studies [78,79], primarily for the delivery of therapeutic proteins and nucleic acids. Drug-loaded MBs may offer the greatest therapeutic benefit by ensuring the simultaneous presence of both the

643 drug and the MBs at the site of action. Nevertheless, their clinical translation is hindered by the need
644 for extensive and costly characterization, as well as rigorous regulatory evaluation prior to approval.
645 Currently, no *in-vivo* comparative investigations have been conducted to evaluate the differences
646 between co-administration or sequential administration of MBs with therapeutic agents and the use
647 of drug-loaded MBs carrying the same agents, or to systematically assess the impact of different
648 administration routes on delivery efficiency and therapeutic outcomes.
649 Recent advances in cochlear gene therapy have further emphasized the need for efficient, safe,
650 and targeted delivery strategies to the inner ear. Several studies have demonstrated the therapeutic
651 potential of adeno-associated viral (AAV) vectors and other genetic modalities for treating SNHL,
652 including approaches aiming to restore hair cell function, promote synaptic repair, or replace
653 defective genes. However, the clinical translation of these strategies remains hindered by the
654 anatomical and physiological barriers of the inner ear—particularly the RWM and the BLB—which
655 limit vector penetration and often require invasive delivery methods. In this context, MB-assisted US
656 emerges as a promising non-invasive or minimally invasive modality capable of enhancing local gene
657 transfer. Recent work has shown that MB cavitation can facilitate AAV passage across the RWM and
658 improve cochlear gene transduction efficiency. These findings support the relevance of integrating
659 MB-assisted US into future gene therapy protocols for hearing restoration. The potential of this
660 combined approach is further reinforced by recent breakthroughs in inner ear gene editing and
661 regeneration strategies, which underline the importance of optimizing delivery tools to enable
662 broader clinical application [89,90].
663 To date, the local administration of MBs—either drug-loaded or co-administered with
664 therapeutic agents—represents the preferred route for the treatment of hearing disorders. Indeed,
665 this mode of administration was employed in 92% of preclinical studies [14,16–21,71,78–81,84]. It includes
666 both direct delivery into the middle ear (used in 75% of recent studies) and transtympanic injection
667 (used in 17% of studies). The choice of this route is largely dictated by the anatomy and
668 vascularization of the inner ear. The inner ear is an anatomically isolated structure and is generally
669 regarded as a poorly vascularized organ relative to other tissues. It is primarily supplied by a single
670 terminal artery—the labyrinthine artery [91,92]. This vascular configuration, which lacks significant
671 collateral circulation, renders the inner ear particularly susceptible to ischemia. Furthermore, the
672 inner ear has a relatively low blood flow, and the presence of the BLB [93] —analogous to the blood-
673 brain barrier—significantly limits the diffusion of therapeutic agents. These characteristics
674 collectively contribute to the challenge of achieving effective pharmacological access to this region.
675 Local administration of MBs and therapeutic agents generally requires surgical intervention to access
676 the target region. However, surgery is not trivial and carries inherent risks, including the potential for
677 infection, localized pain, and facial paralysis if the facial nerve is affected. To overcome these
678 limitations, the intravenous route should be considered a preferable alternative. Indeed, this route
679 represents the simplest and safest clinical approach for administering both MBs and therapeutic
680 agents. To date, only a single preclinical study [83] has successfully demonstrated the use of the
681 intravenous route to treat hearing disorders. Given the limited vascularization of the inner ear,
682 additional preclinical investigations are necessary to validate the relevance and efficacy of
683 intravenous administration. Moreover, it would be highly valuable to conduct comparative preclinical

684 studies assessing local *versus* intravenous delivery in acoustically mediated therapeutic strategies for
685 treatment of hearing disorders. Although most studies investigating RWM sonoporation rely on local
686 administration of MBs and therapeutic agents, a small number of preclinical investigations have used
687 the i.v. route to evaluate whether vascular-accessible MBs can also support US-mediated
688 permeabilization of the RWM. In these studies, the US application site remained strictly focused on
689 the RWM region, and the objective was still to induce transient permeabilization of this membrane.
690 For this reason, i.v. based protocols were included in our analysis, as they offer insight into alternative
691 delivery pathways that may hold relevance for future clinical translation.
692 Interpretation of the *in-vivo* findings must also consider the marked anatomical and
693 physiological differences between animal models. Most available studies were conducted in mice
694 and guinea pigs, whose middle and inner ear structures differ considerably from humans in terms of
695 cochlear size, bone density, and RWM thickness [94]. Such differences can influence US propagation,
696 MB oscillation, and RWM permeability, potentially amplifying the effects observed in small animals
697 compared with the human inner ear. In contrast, the sheep model displays cochlear dimensions,
698 RWM morphology, and middle ear configuration that more closely resemble those of humans,
699 making it a valuable intermediate model for assessing the safety and translational relevance of MB-
700 assisted US [95,96]. These interspecies differences should therefore be taken into account when
701 extrapolating preclinical results to clinical applications.
702 Another important factor influencing the variability of permeabilization outcomes is the lack
703 of systematic evaluation of US parameters. Frequency, peak negative pressure, pulse duration, duty
704 cycle, and total exposure time each exert independent effects on MB oscillation behavior, cavitation
705 thresholds, and the magnitude of microstreaming and shear forces acting on the RWM. These
706 acoustic variables are known to modulate the amplitude and stability of MB oscillations, thereby
707 affecting the extent and reversibility of RWM permeabilization and the subsequent delivery of
708 therapeutic agents. Yet, most preclinical studies rely on empirically selected ultrasound settings, with
709 limited justification or optimization. The absence of standardized acoustic protocols likely
710 contributes to the heterogeneity of reported results and represents a key methodological gap that
711 should be addressed in future investigations. As the aim of the present review was to focus primarily
712 on MB formulations and their biological and pharmacological implications, a detailed analysis of US
713 parameter optimization was beyond its intended scope.
714 Beyond the biological and acoustic considerations, several translational constraints must also
715 be acknowledged. First, most lab-made MB formulations used in preclinical studies are produced
716 with low-throughput methods that lack the scalability and batch-to-batch reproducibility required
717 for clinical-grade manufacturing. Microfluidic technologies enable the production of monodisperse
718 therapeutic MBs but remain costly, technically demanding, and not yet optimized for industrial-scale
719 output. Second, drug-loaded MBs introduce additional manufacturing complexity, as dual-quality
720 control is required for both the carrier and the therapeutic payload, which increases production costs
721 and regulatory burden. Finally, while diagnostic MBs such as SonoVue® and Definity® already benefit
722 from established approval pathways, therapeutic MBs—especially those incorporating drugs, nucleic
723 acids, or proteins—would require full evaluation as novel medicinal products. These constraints

underline the need for streamlined manufacturing processes, improved cost-effectiveness, and early regulatory planning to ensure successful clinical translation of MB-assisted US for inner ear therapies.

Ultimately, a key question in the development of MB-assisted US for drug delivery—particularly concerning MB design to treat hearing disorders is: What are clinicians' expectations regarding therapeutic efficacy? Indeed, therapeutic efficacy objectives remain insufficiently defined in current *in-vitro* and preclinical studies. Establishing these objectives with greater clarity is essential, as the design of therapeutic strategies, US devices, and associated protocols—including both US parameters and MB characteristics—will inevitably vary depending on the intended therapeutic outcomes.

5. FUTURE PERSPECTIVES

Future progress in MB-assisted US for inner ear drug delivery will depend on overcoming several key challenges. First, the substantial heterogeneity in MB formulations, including size distribution, shell viscoelasticity, and surface characteristics, demands systematic optimization to identify MB profiles that maximize safety and therapeutic efficacy. Second, the absence of data describing MB behavior in perilymphatic conditions remains a major knowledge gap, as most mechanistic insights derive from blood-based studies. Third, the lack of standardized US protocols, combined with limited *in-vivo* comparisons of administration routes and delivery strategies, hinders the reproducibility and interpretation of outcomes across studies. In addition, translational implementation will require scalable, cost-effective manufacturing of therapeutic-grade MBs and clear regulatory pathways for drug-loaded formulations. Addressing these challenges through coordinated methodological frameworks, advanced MB engineering, and well-designed comparative preclinical studies will be essential to unlock the full potential of MB-assisted US for future clinical application in otology.

6. CONCLUSION

MB-assisted US represents an innovative and promising modality for the efficient and safe delivery of therapeutic agents to the inner ear for treatment of hearing disorders. Both *in-vitro* and preclinical studies have reported encouraging outcomes regarding the efficacy and safety of this modality. These studies clearly highlight that the physicochemical and pharmacological properties of MBs play a critical role in determining the overall performance and biocompatibility of this modality. The promising results obtained thus far suggest that MB-assisted US has the potential to transform clinical management of inner ear pathologies in the near future. However, further research is needed to establish standardized protocols and to validate the approach using clinically relevant pathological animal models prior to clinical translation.

Funding
This research did not receive any specific grant from funding agencies in the public, commercial, or not-for-profit sectors.

Declaration of Competing Interest
The authors declare that they have no known competing financial interests or personal relationships that could have appeared to influence the work reported in this paper.

Data availability
Data will be made available on request.

Acknowledgments
We thank the House Institute Foundation, Los Angeles, CA, USA for their support.

7. REFERENCES

(1) *Deafness and hearing loss*. https://www.who.int/news-room/fact-sheets/detail/deafness-and-hearing-loss (accessed 2025-03-05).

(2) McDaid, D.; Park, A.-L.; Chadha, S. Estimating the Global Costs of Hearing Loss. *Int. J. Audiol.* **2021**, *60* (3), 162–170. https://doi.org/10.1080/14992027.2021.1883197.

(3) Park, K. Pharmacokinetic Studies for Cochlear Drug Delivery. *J. Controlled Release* **2019**, *299*, 165. https://doi.org/10.1016/j.jconrel.2019.03.007.

(4) Hao, J.; Li, S. K. Inner Ear Drug Delivery: Recent Advances, Challenges, and Perspective. *Eur. J. Pharm. Sci.* **2019**, *126*, 82–92. https://doi.org/10.1016/j.ejps.2018.05.020.

(5) Glueckert, R.; Johnson Chacko, L.; Rask-Andersen, H.; Liu, W.; Handschuh, S.; Schrott-Fischer, A. Anatomical Basis of Drug Delivery to the Inner Ear. *Hear. Res.* **2018**, *368*, 10–27. https://doi.org/10.1016/j.heares.2018.06.017.

(6) Inamura, N.; Salt, A. N. Permeability Changes of the Blood-Labyrinth Barrier Measured in Vivo during Experimental Treatments. *Hear. Res.* **1992**, *61* (1–2), 12–18. https://doi.org/10.1016/0378-5955(92)90030-Q.

(7) *Delivery of Colloidal Particles and Red Blood Cells to Tissue Through Microvessel Ruptures Created by Targeted Microbubble Destruction With Ultrasound*. https://doi.org/10.1161/01.CIR.98.13.1264.

(8) Bouakaz, A.; Zeghimi, A.; Doinikov, A. A. Sonoporation: Concept and Mechanisms. In *Therapeutic Ultrasound*; Escoffre, J.-M., Bouakaz, A., Eds.; Springer International Publishing: Cham, 2016; pp 175–189. https://doi.org/10.1007/978-3-319-22536-4_10.

(9) Escoffre, J.-M.; Bouakaz, A. Minireview: Biophysical Mechanisms of Cell Membrane Sonopermeabilization. Knowns and Unknowns. *Langmuir* **2019**, *35* (31), 10151–10165. https://doi.org/10.1021/acs.langmuir.8b03538.

(10) Pu, C.; Chang, S.; Sun, J.; Zhu, S.; Liu, H.; Zhu, Y.; Wang, Z.; Xu, R. X. Ultrasound-Mediated Destruction of LHRHa-Targeted and Paclitaxel-Loaded Lipid Microbubbles for the Treatment of Intraperitoneal Ovarian Cancer Xenografts. *Mol. Pharm.* **2014**, *11* (1), 49–58. https://doi.org/10.1021/mp400523h.

(11) Lipsman, N.; Meng, Y.; Bethune, A. J.; Huang, Y.; Lam, B.; Masellis, M.; Herrmann, N.; Heyn, C.; Aubert, I.; Boutet, A.; Smith, G. S.; Hynynen, K.; Black, S. E. Blood-Brain Barrier Opening in Alzheimer's Disease Using MR-Guided Focused Ultrasound. *Nat. Commun.* **2018**, *9* (1), 2336. https://doi.org/10.1038/s41467-018-04529-6.

(12) Rix, A.; Curaj, A.; Liehn, E.; Kiessling, F. Ultrasound Microbubbles for Diagnosis and Treatment of Cardiovascular Diseases. *Semin. Thromb. Hemost.* **2020**, *46* (5), 545–552. https://doi.org/10.1055/s-0039-1688492.

(13) Wu, Y.; Deng, C.; Xu, J.; Wang, W.; Chen, Y.; Qin, X.; Lv, Q.; Xie, M. Enhanced Local Delivery of microRNA-145a-5P into Mouse Aorta via Ultrasound-Targeted Microbubble Destruction Inhibits Atherosclerotic Plaque Formation. *Mol. Pharm.* **2023**, *20* (2), 1086–1095. https://doi.org/10.1021/acs.molpharmaceut.2c00799.

(14) Liao, A.-H.; Shi, Z.-P.; Shih, Y.-F.; Chuang, H.-C.; Wang, C.-H. The Application of Ultrasound Enhanced Local Drug Delivery with Albumin Microbubbles in the Inner Ear System. In *2012 IEEE International Ultrasonics Symposium*; 2012; pp 440–443. https://doi.org/10.1109/ULTSYM.2012.0109.

(15) Micaletti, F.; Escoffre, J.-M.; Kerneis, S.; Bouakaz, A.; Galvin, J. J.; Boullaud, L.; Bakhos, D. Microbubble-Assisted Ultrasound for Inner Ear Drug Delivery. *Adv. Drug Deliv. Rev.* **2024**, *204*, 115145. https://doi.org/10.1016/j.addr.2023.115145.
(16) Zhang, Z.; Chen, Z.; Fan, L.; Landry, T.; Brown, J.; Yu, Z.; Yin, S.; Wang, J. Ultrasound-microbubble Cavitation Facilitates Adeno-associated Virus Mediated Cochlear Gene Transfection across the Round-window Membrane. *Bioeng. Transl. Med.* **2020**, *6* (1), e10189. https://doi.org/10.1002/btm2.10189.
(17) Lin, Y.-C.; Chen, H.-C.; Chen, H.-K.; Lin, Y.-Y.; Kuo, C.-Y.; Wang, H.; Hung, C.-L.; Shih, C.-P.; Wang, C.-H. Ultrastructural Changes Associated With the Enhanced Permeability of the Round Window Membrane Mediated by Ultrasound Microbubbles. *Front. Pharmacol.* **2020**, *10*, 1580. https://doi.org/10.3389/fphar.2019.01580.
(18) Shih, C.-P.; Chen, H.-C.; Chen, H.-K.; Chiang, M.-C.; Sytwu, H.-K.; Lin, Y.-C.; Li, S.-L.; Shih, Y.-F.; Liao, A.-H.; Wang, C.-H. Ultrasound-Aided Microbubbles Facilitate the Delivery of Drugs to the Inner Ear via the Round Window Membrane. *J. Controlled Release* **2013**, *167* (2), 167–174. https://doi.org/10.1016/j.jconrel.2013.01.028.
(19) Lin, Y.-C.; Shih, C.-P.; Chen, H.-C.; Chou, Y.-L.; Sytwu, H.-K.; Fang, M.-C.; Lin, Y.-Y.; Kuo, C.-Y.; Su, H.-H.; Hung, C.-L.; Chen, H.-K.; Wang, C.-H. Ultrasound Microbubble–Facilitated Inner Ear Delivery of Gold Nanoparticles Involves Transient Disruption of the Tight Junction Barrier in the Round Window Membrane. *Front. Pharmacol.* **2021**, *12*, 689032. https://doi.org/10.3389/fphar.2021.689032.
(20) Kerneis, S.; Escoffre, J.-M.; Galvin, J. J.; Bouakaz, A.; Presset, A.; Alix, C.; Oujagir, E.; Lefèvre, A.; Emond, P.; Blasco, H.; Bakhos, D. Sonoporation of the Round Window Membrane on a Sheep Model: A Safety Study. *Pharmaceutics* **2023**, *15* (2), 442. https://doi.org/10.3390/pharmaceutics15020442.
(21) Liao, A.-H.; Shih, C.-P.; Li, M.-W.; Lin, Y.-C.; Chuang, H.-C.; Wang, C.-H. Development of Thermosensitive Poloxamer 407-Based Microbubble Gel with Ultrasound Mediation for Inner Ear Drug Delivery. *Drug Deliv.* **2021**, *28* (1), 1256–1271. https://doi.org/10.1080/10717544.2021.1938758.
(22) Kamaev, P. P.; Hutcheson, J. D.; Wilson, M. L.; Prausnitz, M. R. Quantification of Optison Bubble Size and Lifetime during Sonication Dominant Role of Secondary Cavitation Bubbles Causing Acoustic Bioeffects. *J. Acoust. Soc. Am.* **2004**, *115* (4), 1818–1825. https://doi.org/10.1121/1.1624073.
(23) Azmin, M.; Harfield, C.; Ahmad, Z.; Edirisinghe, M.; Stride, E. How Do Microbubbles and Ultrasound Interact? Basic Physical, Dynamic and Engineering Principles. *Curr. Pharm. Des.* **2012**, *18* (15), 2118–2134. https://doi.org/10.2174/138161212800099955.
(24) Moher, D.; Liberati, A.; Tetzlaff, J.; Altman, D. Moher D, Liberati A, Tetzlaff J, Altman DG, Group PPreferred Reporting Items for Systematic Reviews and Meta-Analyses: The PRISMA Statement. PLoS Med 6: E1000097. *Open Med. Peer-Rev. Indep. Open-Access J.* **2009**, *3*, e123-30. https://doi.org/10.1016/j.jclinepi.2009.06.005.
(25) Yang, Y.; Liu, Y.; Jiang, Y. Recent Advances in Perfluorocarbon-Based Delivery Systems for Cancer Theranostics. *Mol. Pharm.* **2023**, *20* (7), 3254–3277. https://doi.org/10.1021/acs.molpharmaceut.3c00116.
(26) Kwan, J. J.; Borden, M. A. Microbubble Dissolution in a Multigas Environment. *Langmuir ACS J. Surf. Colloids* **2010**, *26* (9), 6542–6548. https://doi.org/10.1021/la904088p.
(27) Porter, T.; Kricsfeld, D.; Cheatham, S.; Li, S. Effect of Blood and Microbubble Oxygen and Nitrogen Content on Perfluorocarbon-Filled Dextrose Albumin Microbubble Size and

Efficacy: In Vitro and in Vivo Studies. *J. Am. Soc. Echocardiogr. Off. Publ. Am. Soc. Echocardiogr.* **1998**, *11* (5), 421–425. https://doi.org/10.1016/s0894-7317(98)70020-3.
(28) Ho, Y.-J.; Chu, S.-W.; Liao, E.-C.; Fan, C.-H.; Chan, H.-L.; Wei, K.-C.; Yeh, C.-K. Normalization of Tumor Vasculature by Oxygen Microbubbles with Ultrasound. *Theranostics* **2019**, *9* (24), 7370–7383. https://doi.org/10.7150/thno.37750.
(29) Upadhyay, A.; Dalvi, S. V.; Gupta, G.; Khanna, N. Effect of PEGylation on Performance of Protein Microbubbles and Its Comparison with Lipid Microbubbles. *Mater. Sci. Eng. C* **2017**, *71*, 425–430. https://doi.org/10.1016/j.msec.2016.10.021.
(30) Cavalieri, F.; Ashokkumar, M.; Grieser, F.; Caruso, F. Ultrasonic Synthesis of Stable, Functional Lysozyme Microbubbles. *Langmuir ACS J. Surf. Colloids* **2008**, *24* (18), 10078–10083. https://doi.org/10.1021/la801093q.
(31) Lozano, M. M.; Longo, M. L. Microbubbles Coated with Disaturated Lipids and DSPE-PEG2000: Phase Behavior, Collapse Transitions, and Permeability. *Langmuir ACS J. Surf. Colloids* **2009**, *25* (6), 3705–3712. https://doi.org/10.1021/la803774q.
(32) Angilè, F. E.; Vargo, K. B.; Sehgal, C. M.; Hammer, D. A.; Lee, D. Recombinant Protein-Stabilized Monodisperse Microbubbles with Tunable Size Using a Valve-Based Microfluidic Device. *Langmuir* **2014**, *30* (42), 12610–12618. https://doi.org/10.1021/la502610c.
(33) Navarro-Becerra, J. A.; Borden, M. A. Targeted Microbubbles for Drug, Gene, and Cell Delivery in Therapy and Immunotherapy. *Pharmaceutics* **2023**, *15* (6), 1625. https://doi.org/10.3390/pharmaceutics15061625.
(34) Owen, J.; Crake, C.; Lee, J. Y.; Carugo, D.; Beguin, E.; Khrapitchev, A. A.; Browning, R. J.; Sibson, N.; Stride, E. A Versatile Method for the Preparation of Particle-Loaded Microbubbles for Multimodality Imaging and Targeted Drug Delivery. *Drug Deliv. Transl. Res.* **2018**, *8* (2), 342–356. https://doi.org/10.1007/s13346-017-0366-7.
(35) Katiyar, A.; Sarkar, K.; Jain, P. Effects of Encapsulation Elasticity on the Stability of an Encapsulated Microbubble. *J. Colloid Interface Sci.* **2009**, *336* (2), 519–525. https://doi.org/10.1016/j.jcis.2009.05.019.
(36) Borden, M. A.; Kruse, D. E.; Caskey, C. F.; Zhao, S.; Dayton, P. A.; Ferrara, K. W. Influence of Lipid Shell Physicochemical Properties on Ultrasound-Induced Microbubble Destruction. *IEEE Trans. Ultrason. Ferroelectr. Freq. Control* **2005**, *52* (11), 1992–2002. https://doi.org/10.1109/TUFFC.2005.1561668.
(37) *Drug Loading in Poly(butyl cyanoacrylate)-Based Polymeric Microbubbles | Molecular Pharmaceutics*. https://pubs.acs.org/doi/10.1021/acs.molpharmaceut.0c00242 (accessed 2025-03-06).
(38) Xiong, X.; Zhao, F.; Shi, M.; Yang, H.; Liu, Y. Polymeric Microbubbles for Ultrasonic Molecular Imaging and Targeted Therapeutics. *J. Biomater. Sci. Polym. Ed.* **2011**, *22* (4–6), 417–428. https://doi.org/10.1163/092050610X540440.
(39) Rudakovskaya, P. G.; Barmin, R. A.; Kuzmin, P. S.; Fedotkina, E. P.; Sencha, A. N.; Gorin, D. A. Microbubbles Stabilized by Protein Shell: From Pioneering Ultrasound Contrast Agents to Advanced Theranostic Systems. *Pharmaceutics* **2022**, *14* (6), 1236. https://doi.org/10.3390/pharmaceutics14061236.
(40) Sirsi, S.; Borden, M. Microbubble Compositions, Properties and Biomedical Applications. *Bubble Sci. Eng. Technol.* **2009**, *1* (1–2), 3–17. https://doi.org/10.1179/175889709X446507.
(41) Ja'afar, F.; Leow, C. H.; Garbin, V.; Sennoga, C. A.; Tang, M.-X.; Seddon, J. M. Surface Charge Measurement of SonoVue, Definity and Optison: A Comparison of Laser Doppler

Electrophoresis and Micro-Electrophoresis. *Ultrasound Med. Biol.* **2015**, *41* (11), 2990–3000. https://doi.org/10.1016/j.ultrasmedbio.2015.07.001.

(42) Zhong, Y.; Guo, T.; Dong, F.; Zhang, J. Effect of Surface Charge Modification on the Imaging Performance of Targeted Microbubbles. In *2024 IEEE Ultrasonics, Ferroelectrics, and Frequency Control Joint Symposium (UFFC-JS)*; 2024; pp 1–3. https://doi.org/10.1109/UFFC-JS60046.2024.10793504.

(43) Zhou, Y.; Gu, H.; Xu, Y.; Li, F.; Kuang, S.; Wang, Z.; Zhou, X.; Ma, H.; Li, P.; Zheng, Y.; Ran, H.; Jian, J.; Zhao, Y.; Song, W.; Wang, Q.; Wang, D. Targeted Antiangiogenesis Gene Therapy Using Targeted Cationic Microbubbles Conjugated with CD105 Antibody Compared with Untargeted Cationic and Neutral Microbubbles. *Theranostics* **2015**, *5* (4), 399–417. https://doi.org/10.7150/thno.10351.

(44) Yin, J.; Dong, F.; An, J.; Guo, T.; Cheng, H.; Zhang, J.; Zhang, J. Pattern Recognition of Microcirculation with Super-Resolution Ultrasound Imaging Provides Markers for Early Tumor Response to Anti-Angiogenic Therapy. *Theranostics* **2024**, *14* (3), 1312–1324. https://doi.org/10.7150/thno.89306.

(45) Xie, A.; Belcik, T.; Qi, Y.; Morgan, T. K.; Champaneri, S. A.; Taylor, S.; Davidson, B. P.; Zhao, Y.; Klibanov, A. L.; Kuliszewski, M. A.; Leong-Poi, H.; Ammi, A.; Lindner, J. R. Ultrasound-Mediated Vascular Gene Transfection by Cavitation of Endothelial-Targeted Cationic Microbubbles. *JACC Cardiovasc. Imaging* **2012**, *5* (12), 1253–1262. https://doi.org/10.1016/j.jcmg.2012.05.017.

(46) Fisher, N. G.; Christiansen, J. P.; Klibanov, A.; Taylor, R. P.; Kaul, S.; Lindner, J. R. Influence of Microbubble Surface Charge on Capillary Transit and Myocardial Contrast Enhancement. *J. Am. Coll. Cardiol.* **2002**, *40* (4), 811–819. https://doi.org/10.1016/S0735-1097(02)02038-7.

(47) Tinkov, S.; Winter, G.; Coester, C.; Bekeredjian, R. New Doxorubicin-Loaded Phospholipid Microbubbles for Targeted Tumor Therapy: Part I--Formulation Development and in-Vitro Characterization. *J. Control. Release Off. J. Control. Release Soc.* **2010**, *143* (1), 143–150. https://doi.org/10.1016/j.jconrel.2009.12.026.

(48) Kooiman, K.; Böhmer, M. R.; Emmer, M.; Vos, H. J.; Chlon, C.; Shi, W. T.; Hall, C. S.; de Winter, S. H. P. M.; Schroën, K.; Versluis, M.; de Jong, N.; van Wamel, A. Oil-Filled Polymer Microcapsules for Ultrasound-Mediated Delivery of Lipophilic Drugs. *J. Control. Release Off. J. Control. Release Soc.* **2009**, *133* (2), 109–118. https://doi.org/10.1016/j.jconrel.2008.09.085.

(49) Böhmer, M. R.; Klibanov, A. L.; Tiemann, K.; Hall, C. S.; Gruell, H.; Steinbach, O. C. Ultrasound Triggered Image-Guided Drug Delivery. *Eur. J. Radiol.* **2009**, *70* (2), 242–253. https://doi.org/10.1016/j.ejrad.2009.01.051.

(50) Borden, M. A.; Caskey, C. F.; Little, E.; Gillies, R. J.; Ferrara, K. W. DNA and Polylysine Adsorption and Multilayer Construction onto Cationic Lipid-Coated Microbubbles. *Langmuir ACS J. Surf. Colloids* **2007**, *23* (18), 9401–9408. https://doi.org/10.1021/la7009034.

(51) Sirsi, S. R.; Borden, M. A. Advances in Ultrasound Mediated Gene Therapy Using Microbubble Contrast Agents. *Theranostics* **2012**, *2* (12), 1208–1222. https://doi.org/10.7150/thno.4306.

(52) Fournier, L.; Abioui-Mourgues, M.; Chabouh, G.; Aid, R.; Taille, T. D. L.; Couture, O.; Vivien, D.; Orset, C.; Chauvierre, C. rtPA-Loaded Fucoidan Polymer Microbubbles for the Targeted Treatment of Stroke. *Biomaterials* **2023**, *303*, 122385. https://doi.org/10.1016/j.biomaterials.2023.122385.

(53) Bouakaz, A.; Michel Escoffre, J. From Concept to Early Clinical Trials: 30 Years of Microbubble-Based Ultrasound-Mediated Drug Delivery Research. *Adv. Drug Deliv. Rev.* **2024**, *206*, 115199. https://doi.org/10.1016/j.addr.2024.115199.
(54) Sennoga, C. A.; Kanbar, E.; Auboire, L.; Dujardin, P.-A.; Fouan, D.; Escoffre, J.-M.; Bouakaz, A. Microbubble-Mediated Ultrasound Drug-Delivery and Therapeutic Monitoring. *Expert Opin. Drug Deliv.* **2017**, *14* (9), 1031–1043. https://doi.org/10.1080/17425247.2017.1266328.
(55) *Ultrasound-Responsive Cavitation Nuclei for Therapy and Drug Delivery - Ultrasound in Medicine and Biology*. https://www.umbjournal.org/article/S0301-5629(20)30004-1/fulltext (accessed 2025-05-05).
(56) Supponen, O.; Upadhyay, A.; Lum, J.; Guidi, F.; Murray, T.; Vos, H. J.; Tortoli, P.; Borden, M. The Effect of Size Range on Ultrasound-Induced Translations in Microbubble Populations. *J. Acoust. Soc. Am.* **2020**, *147* (5), 3236. https://doi.org/10.1121/10.0001172.
(57) Chomas, J. E.; Dayton, P.; May, D.; Ferrara, K. Threshold of Fragmentation for Ultrasonic Contrast Agents. *J. Biomed. Opt.* **2001**, *6* (2), 141–150. https://doi.org/10.1117/1.1352752.
(58) Zheng, H.; Dayton, P. A.; Caskey, C.; Zhao, S.; Qin, S.; Ferrara, K. W. Ultrasound-Driven Microbubble Oscillation and Translation within Small Phantom Vessels. *Ultrasound Med. Biol.* **2007**, *33* (12), 1978–1987. https://doi.org/10.1016/j.ultrasmedbio.2007.06.007.
(59) Qin, S.; Ferrara, K. W. The Natural Frequency of Nonlinear Oscillation of Ultrasound Contrast Agents in Microvessels. *Ultrasound Med. Biol.* **2007**, *33* (7), 1140–1148. https://doi.org/10.1016/j.ultrasmedbio.2006.12.009.
(60) Kooiman, K.; Vos, H. J.; Versluis, M.; de Jong, N. Acoustic Behavior of Microbubbles and Implications for Drug Delivery. *Adv. Drug Deliv. Rev.* **2014**, *72*, 28–48. https://doi.org/10.1016/j.addr.2014.03.003.
(61) Matalliotakis, A.; Verweij, M. D. Polydisperse Versus Monodisperse Microbubbles: A Simulation Study for Contrast-Enhanced Ultrasound Imaging. *Ultrasound Med. Biol.* **2025**, *51* (3), 452–462. https://doi.org/10.1016/j.ultrasmedbio.2024.11.002.
(62) van Elburg, B.; Deprez, J.; van den Broek, M.; De Smedt, S. C.; Versluis, M.; Lajoinie, G.; Lentacker, I.; Segers, T. Dependence of Sonoporation Efficiency on Microbubble Size: An in Vitro Monodisperse Microbubble Study. *J. Controlled Release* **2023**, *363*, 747–755. https://doi.org/10.1016/j.jconrel.2023.09.047.
(63) Choi, J. J.; Feshitan, J. A.; Baseri, B.; Wang, S.; Tung, Y.-S.; Borden, M. A.; Konofagou, E. E. Microbubble-Size Dependence of Focused Ultrasound-Induced Blood–Brain Barrier Opening in Mice In Vivo. *IEEE Trans. Biomed. Eng.* **2010**, *57* (1), 145–154. https://doi.org/10.1109/TBME.2009.2034533.
(64) Wang, Y.; Li, H.; Meijlink, B.; Luo, J.; Beurskens, R.; Johnson, B.; Kooiman, K. Monodisperse Microbubble-Mediated Drug Delivery: Influence of Microbubbles Size on Drug Delivery Outcome. *J. Acoust. Soc. Am.* **2024**, *155* (3_Supplement), A325. https://doi.org/10.1121/10.0027679.
(65) Lentacker, I.; Geers, B.; Demeester, J.; De Smedt, S. C.; Sanders, N. N. Design and Evaluation of Doxorubicin-Containing Microbubbles for Ultrasound-Triggered Doxorubicin Delivery: Cytotoxicity and Mechanisms Involved. *Mol. Ther. J. Am. Soc. Gene Ther.* **2010**, *18* (1), 101–108. https://doi.org/10.1038/mt.2009.160.
(66) Lammertink, B. H. A.; Bos, C.; van der Wurff-Jacobs, K. M.; Storm, G.; Moonen, C. T.; Deckers, R. Increase of Intracellular Cisplatin Levels and Radiosensitization by Ultrasound in Combination with Microbubbles. *J. Control. Release Off. J. Control. Release Soc.* **2016**, *238*, 157–165. https://doi.org/10.1016/j.jconrel.2016.07.049.

(67) Roy, M.; Alix, C.; Burlaud-Gaillard, J.; Fouan, D.; Raoul, W.; Bouakaz, A.; Blanchard, E.; Lecomte, T.; Viaud-Massuard, M.-C.; Sasaki, N.; Serrière, S.; Escoffre, J.-M. Delivery of Anticancer Drugs Using Microbubble-Assisted Ultrasound in a 3D Spheroid Model. *Mol. Pharm.* **2024**, *21* (2), 831–844. https://doi.org/10.1021/acs.molpharmaceut.3c00921.
(68) Bourn, M. D.; Batchelor, D. V. B.; Ingram, N.; McLaughlan, J. R.; Coletta, P. L.; Evans, S. D.; Peyman, S. A. High-Throughput Microfluidics for Evaluating Microbubble Enhanced Delivery of Cancer Therapeutics in Spheroid Cultures. *J. Control. Release Off. J. Control. Release Soc.* **2020**, *326*, 13–24. https://doi.org/10.1016/j.jconrel.2020.06.011.
(69) Kopechek, J. A.; McTiernan, C. F.; Chen, X.; Zhu, J.; Mburu, M.; Feroze, R.; Whitehurst, D. A.; Lavery, L.; Cyriac, J.; Villanueva, F. S. Ultrasound and Microbubble-Targeted Delivery of a microRNA Inhibitor to the Heart Suppresses Cardiac Hypertrophy and Preserves Cardiac Function. *Theranostics* **2019**, *9* (23), 7088–7098. https://doi.org/10.7150/thno.34895.
(70) Sugiyama, M. G.; Mintsopoulos, V.; Raheel, H.; Goldenberg, N. M.; Batt, J. E.; Brochard, L.; Kuebler, W. M.; Leong-Poi, H.; Karshafian, R.; Lee, W. L. Lung Ultrasound and Microbubbles Enhance Aminoglycoside Efficacy and Delivery to the Lung in Escherichia Coli-Induced Pneumonia and Acute Respiratory Distress Syndrome. *Am. J. Respir. Crit. Care Med.* **2018**, *198* (3), 404–408. https://doi.org/10.1164/rccm.201711-2259LE.
(71) Shih, C.-P.; Chen, H.-C.; Lin, Y.-C.; Chen, H.-K.; Wang, H.; Kuo, C.-Y.; Lin, Y.-Y.; Wang, C.-H. Middle-Ear Dexamethasone Delivery via Ultrasound Microbubbles Attenuates Noise-Induced Hearing Loss. *The Laryngoscope* **2019**, *129* (8), 1907–1914. https://doi.org/10.1002/lary.27713.
(72) Sonabend, A. M.; Gould, A.; Amidei, C.; Ward, R.; Schmidt, K. A.; Zhang, D. Y.; Gomez, C.; Bebawy, J. F.; Liu, B. P.; Bouchoux, G.; Desseaux, C.; Helenowski, I. B.; Lukas, R. V.; Dixit, K.; Kumthekar, P.; Arrieta, V. A.; Lesniak, M. S.; Carpentier, A.; Zhang, H.; Muzzio, M.; Canney, M.; Stupp, R. Repeated Blood-Brain Barrier Opening with an Implantable Ultrasound Device for Delivery of Albumin-Bound Paclitaxel in Patients with Recurrent Glioblastoma: A Phase 1 Trial. *Lancet Oncol.* **2023**, *24* (5), 509–522. https://doi.org/10.1016/S1470-2045(23)00112-2.
(73) Haram, M.; Hansen, R.; Bouget, D.; Myhre, O. F.; Davies, C. de L.; Hofsli, E. Treatment of Liver Metastases With Focused Ultrasound and Microbubbles in Patients With Colorectal Cancer Receiving Chemotherapy. *Ultrasound Med. Biol.* **2023**, *49* (9), 2081–2088. https://doi.org/10.1016/j.ultrasmedbio.2023.05.013.
(74) Bae, S.; Liu, K.; Pouliopoulos, A. N.; Ji, R.; Jiménez-Gambín, S.; Yousefian, O.; Kline-Schoder, A. R.; Batts, A. J.; Tsitsos, F. N.; Kokossis, D.; Mintz, A.; Honig, L. S.; Konofagou, E. E. Transcranial Blood-Brain Barrier Opening in Alzheimer's Disease Patients Using a Portable Focused Ultrasound System with Real-Time 2-D Cavitation Mapping. *Theranostics* **2024**, *14* (11), 4519–4535. https://doi.org/10.7150/thno.94206.
(75) Ilovitsh, T.; Feng, Y.; Foiret, J.; Kheirolomoom, A.; Zhang, H.; Ingham, E. S.; Ilovitsh, A.; Tumbale, S. K.; Fite, B. Z.; Wu, B.; Raie, M. N.; Zhang, N.; Kare, A. J.; Chavez, M.; Qi, L. S.; Pelled, G.; Gazit, D.; Vermesh, O.; Steinberg, I.; Gambhir, S. S.; Ferrara, K. W. Low-Frequency Ultrasound-Mediated Cytokine Transfection Enhances T Cell Recruitment at Local and Distant Tumor Sites. *Proc. Natl. Acad. Sci. U. S. A.* **2020**, *117* (23), 12674–12685. https://doi.org/10.1073/pnas.1914906117.
(76) Kobulnik, J.; Kuliszewski, M. A.; Stewart, D. J.; Lindner, J. R.; Leong-Poi, H. Comparison of Gene Delivery Techniques for Therapeutic Angiogenesis Ultrasound-Mediated Destruction of Carrier Microbubbles versus Direct Intramuscular Injection. *J. Am. Coll. Cardiol.* **2009**, *54* (18), 1735–1742. https://doi.org/10.1016/j.jacc.2009.07.023.

(77) Weiser, J. R.; Saltzman, W. M. Controlled Release for Local Delivery of Drugs: Barriers and Models. *J. Control. Release Off. J. Control. Release Soc.* **2014**, *190*, 664–673. https://doi.org/10.1016/j.jconrel.2014.04.048.
(78) Lin, Y.-Y.; Liao, A.-H.; Li, H.-T.; Jiang, P.-Y.; Lin, Y.-C.; Chuang, H.-C.; Ma, K.-H.; Chen, H.-K.; Liu, Y.-T.; Shih, C.-P.; Wang, C.-H. Ultrasound-Mediated Lysozyme Microbubbles Targeting NOX4 Knockdown Alleviate Cisplatin-Exposed Cochlear Hair Cell Ototoxicity. *Int. J. Mol. Sci.* **2024**, *25* (13), 7096. https://doi.org/10.3390/ijms25137096.
(79) Liao, A.-H.; Wang, C.-H.; Wang, B.-H.; Lin, Y.-C.; Chuang, H.-C.; Liu, H.-L.; Shih, C.-P. Combined Use of Microbubbles of Various Sizes and Single-Transducer Dual-Frequency Ultrasound for Safe and Efficient Inner Ear Drug Delivery. *Bioeng. Transl. Med.* **2022**, *8* (5), e10450. https://doi.org/10.1002/btm2.10450.
(80) Liao, A.-H.; Wang, C.-H.; Weng, P.-Y.; Lin, Y.-C.; Wang, H.; Chen, H.-K.; Liu, H.-L.; Chuang, H.-C.; Shih, C.-P. Ultrasound-Induced Microbubble Cavitation via a Transcanal or Transcranial Approach Facilitates Inner Ear Drug Delivery. *JCI Insight* **2020**, *5* (3), e132880. https://doi.org/10.1172/jci.insight.132880.
(81) Liao, A.-H.; Hsieh, Y.-L.; Ho, H.-C.; Chen, H.-K.; Lin, Y.-C.; Shih, C.-P.; Chen, H.-C.; Kuo, C.-Y.; Lu, Y.-J.; Wang, C.-H. Effects of Microbubble Size on Ultrasound-Mediated Gene Transfection in Auditory Cells. *BioMed Res. Int.* **2014**, *2014*, 840852. https://doi.org/10.1155/2014/840852.
(82) Nomikou, N.; Tiwari, P.; Trehan, T.; Gulati, K.; McHale, A. P. Studies on Neutral, Cationic and Biotinylated Cationic Microbubbles in Enhancing Ultrasound-Mediated Gene Delivery in Vitro and in Vivo. *Acta Biomater.* **2012**, *8* (3), 1273–1280. https://doi.org/10.1016/j.actbio.2011.09.010.
(83) He, Y.; Chen, Z.; Liu, Q.; Li, Z.; Wen, D.; Zhang, H.; Zhang, M.; Jiang, D.; Li, H.; Wen, L.; Chen, G. Reversible Opening of the Blood-Labyrinth Barrier by Low-Pressure Pulsed Ultrasound and Microbubbles for the Treatment of Inner Ear Diseases. *J. Controlled Release* **2024**, *372*, 318–330. https://doi.org/10.1016/j.jconrel.2024.06.043.
(84) Lin, Y.-C.; Lin, Y.-Y.; Chen, H.-C.; Kuo, C.-Y.; Liao, A.-H.; Chou, Y.-L.; Hung, C.-L.; Shih, C.-P.; Wang, C.-H. Ultrasound Microbubbles Enhance the Efficacy of Insulin-Like Growth Factor-1 Therapy for the Treatment of Noise-Induced Hearing Loss. *Molecules* **2021**, *26* (12), 3626. https://doi.org/10.3390/molecules26123626.
(85) Shi, D.; Guo, L.; Duan, S.; Shang, M.; Meng, D.; Cheng, L.; Li, J. Influence of Tumor Cell Lines Derived from Different Tissue on Sonoporation Efficiency under Ultrasound Microbubble Treatment. *Ultrason. Sonochem.* **2017**, *38*, 598–603. https://doi.org/10.1016/j.ultsonch.2016.08.022.
(86) Miller, D. L.; Quddus, J. Sonoporation of Monolayer Cells by Diagnostic Ultrasound Activation of Contrast-Agent Gas Bodies. *Ultrasound Med. Biol.* **2000**, *26* (4), 661–667. https://doi.org/10.1016/s0301-5629(99)00170-2.
(87) Xu, X.; Chen, H.; Wu, X.; Chen, S.; Qi, J.; He, Z.; Zou, S.; Xie, L.; Xu, K.; Yuan, H.; Sun, Y.; Zheng, H.; Kong, W. Hollow Mesoporous Silica@Zeolitic Imidazolate Framework Capsules and Their Applications for Gentamicin Delivery. *Neural Plast.* **2018**, *2018*, 2160854. https://doi.org/10.1155/2018/2160854.
(88) *A metal–organic framework based inner ear delivery system for the treatment of noise-induced hearing loss - Nanoscale (RSC Publishing)*. https://pubs.rsc.org/en/content/articlelanding/2020/nr/d0nr04860g (accessed 2025-11-30).

(89) Lv, J.; Wang, H.; Cheng, X.; Chen, Y.; Wang, D.; Zhang, L.; Cao, Q.; Tang, H.; Hu, S.; Gao, K.; Xun, M.; Wang, J.; Wang, Z.; Zhu, B.; Cui, C.; Gao, Z.; Guo, L.; Yu, S.; Jiang, L.; Yin, Y.; Zhang, J.; Chen, B.; Wang, W.; Chai, R.; Chen, Z.-Y.; Li, H.; Shu, Y. AAV1-hOTOF Gene Therapy for Autosomal Recessive Deafness 9: A Single-Arm Trial. *The Lancet* **2024**, *403* (10441), 2317–2325. https://doi.org/10.1016/S0140-6736(23)02874-X.

(90) Wang, X.; Zhang, L.; Chen, S.; Xie, L.; Qiu, Y.; Kong, C.; Yin, G.; Kong, W.; Sun, Y. Viral-Mediated Connexin 26 Expression Combined with Dexamethasone Rescues Hearing in a Conditional Gjb2 Null Mice Model. *Adv. Sci.* **2025**, *12* (29), 2406510. https://doi.org/10.1002/advs.202406510.

(91) Masson, E. *Anatomie de l'oreille interne*. EM-Consulte. https://www.em-consulte.com/article/1179/anatomie-de-l-oreille-interne (accessed 2025-07-12).

(92) Bruss, D. M.; Shohet, J. A. Neuroanatomy, Ear. In *StatPearls*; StatPearls Publishing: Treasure Island (FL), 2025.

(93) Yi, Z.; Wang, X.; Yin, G.; Sun, Y. The Blood-Labyrinth Barrier: Non-Invasive Delivery Strategies for Inner Ear Drug Delivery. *Pharmaceutics* **2025**, *17* (4), 482. https://doi.org/10.3390/pharmaceutics17040482.

(94) Thorne, M.; Salt, A. N.; DeMott, J. E.; Henson, M. M.; Henson, O. W.; Gewalt, S. L. Cochlear Fluid Space Dimensions for Six Species Derived from Reconstructions of Three-Dimensional Magnetic Resonance Images. *The Laryngoscope* **1999**, *109* (10), 1661–1668. https://doi.org/10.1097/00005537-199910000-00021.

(95) Lue, P.-Y.; Oliver, M. H.; Neeff, M.; Thorne, P. R.; Suzuki-Kerr, H. Sheep as a Large Animal Model for Hearing Research: Comparison to Common Laboratory Animals and Humans. *Lab. Anim. Res.* **2023**, *39* (1), 31. https://doi.org/10.1186/s42826-023-00182-3.

(96) Trinh, T.-T.; Cohen, C.; Boullaud, L.; Cottier, J. P.; Bakhos, D. Sheep as a Large Animal Model for Cochlear Implantation. *Braz. J. Otorhinolaryngol.* **2021**, *88* (Suppl 1), S24–S32. https://doi.org/10.1016/j.bjorl.2021.02.014.